

1 Flood risk assessment for Indian sub-continental river basins

2 Urmin Vegad¹, Yadu Pokhrel², and Vimal Mishra^{1,3*}

3

4 ¹Civil Engineering, Indian Institute of Technology (IIT) Gandhinagar

5 ²[Department of Civil and Environmental Engineering, Michigan State University, East Lansing, Michigan, USA](#)

Deleted: ²Civil

6 ³Earth Sciences, Indian Institute of Technology (IIT) Gandhinagar

7 *Corresponding author: vmishra@iitgn.ac.in

8 Abstract

9 Floods are among India's most frequently occurring natural disasters, which disrupt all aspects of socio-economic
10 well-being. A large population is affected by floods during almost every summer monsoon season in India, leaving
11 its footprint through human mortality, migration, and damage to agriculture and infrastructure. Despite the
12 massive imprints of floods, sub-basin level flood risk assessment is still in its infancy and [requires advancements](#).
13 Using hydrological and hydrodynamical models, we reconstructed sub-basin level observed floods for the 1901-
14 2020 period. Our modelling framework includes the influence of 51 major reservoirs that affect flow variability
15 and flood inundation. Sub-basins in the Ganga and Brahmaputra River basins witnessed [substantial](#) flood
16 [inundation](#) extent during the worst flood in the observational record. Major floods in the sub-basins of the Ganga
17 and Brahmaputra occur during the late summer monsoon season (August-September). Beas, Brahmani, upper
18 Satluj, Upper Godavari, Middle and Lower Krishna, and Vashishti sub-basins are among the most influenced by
19 the dams, while Beas, Brahmani, Ravi, and Lower Satluj are among the most impacted by floods and the presence
20 of dams. Bhagirathi, Gandak, Kosi, lower Brahmaputra, and Ghaghara are India's sub-basins with the highest
21 flood risk. Our findings have implications for flood [risk assessment and](#) mitigation in India.

Deleted: needs to be improved.

Deleted: the greatest

22 1. Introduction

23 Flood risk to both natural and human systems is projected to increase due to climate change (IPCC, 2014, 2022).
24 Extreme weather and climate extremes have increased under warming climate, leading to an increased frequency
25 of natural hazards like floods, droughts, heat waves, cyclones, and heavy rains. Hydroclimatic extremes affect
26 humans and infrastructure (Eidsvig et al., 2017; Peduzzi et al., 2009). Due to high vulnerability and lower adaptive
27 capacity, developing countries are often the most impacted by extreme weather events. Further, developing
28 countries usually take longer to recover from the hazards due to low climate resilience. Globally, floods are among
29 the most devastating natural hazards (Ghosh & Kar, 2018). Among all flood types, riverine floods occur most
30 frequently (Kimuli et al., 2021) and often cause substantial damage to agriculture and infrastructure. A
31 considerable fraction of the population and infrastructure are exposed to flooding, which will also increase due to
32 the projected increase in the magnitude and frequency of floods (Winsemius et al., 2018).

Deleted:

Formatted: Font: 11 pt

33 The increase in flood magnitude due to the warming climate has resulted in considerable economic losses (C. M.
34 R. Mateo et al., 2014; Willner et al., 2018). The total financial loss will likely increase by 17% in the next 20 years
35 due to climate change (Willner et al., 2018). Besides agriculture, floods significantly affect the built environment
36 and transportation infrastructure (Kalantari et al., 2014). For instance, more than 7% of road and railway assets

41 globally are exposed to a 100-year return period flood (Koks et al., 2019). In Asia, about 75% of the population
42 is exposed to riverine floods (Varis et al., 2022). India falls among the top ten most flood-affected countries in
43 Asia and the Pacific (Kimuli et al., 2021). In addition, India is also among the top-ten countries that experienced
44 the highest human mortality due to floods. Considerable population exposure, climate change, and rapid growth
45 and development in flood-prone areas contribute to increased losses from floods.

46 In India, state administration takes decisions to mitigate floods while the central government provides financial
47 aid under severe conditions (Jain et al., 2017). The state authorities develop action plans to minimize flood
48 damage. Therefore, identifying the regions with higher flood risk is essential for planning and mitigation. Flood
49 impacts can be quantified according to the affected population, gross domestic product (GDP), and agricultural
50 practices (Ward et al., 2013). The flood risk assessment framework suggested by the Intergovernmental Panel on
51 Climate Change (IPCC) has been extensively applied at the regional and global scales (Allen et al., 2016; IPCC,
52 2014; Roy et al., 2021). The risk can be quantified as a function of vulnerability, hazard, and exposure (IPCC,
53 2014). To control the risk, reducing vulnerability is considered a short to the mid-term goal (V. Mishra et al.,
54 2022), while reducing hazards and exposure are long-term goals (Birkmann & Welle, 2015). Flood risk
55 assessment can assist in identifying the regions at high risk due to higher vulnerability, hazard, and exposure,
56 which can be used for developing a framework, methodology, and guidelines for flood mitigation and damage
57 assessment.

58 A flood risk assessment performed on a global scale may not help in identifying the flood risk-prone regions at a
59 country scale due to the coarser spatial resolution (Bernhofen et al., 2022). Due to complex geomorphological
60 characteristics and diverse climatic conditions, India is considered a relatively high flood-risk region (Hochrainer-
61 Stigler et al., 2021). Therefore, estimating flood risk on a finer scale (e.g. sub-basin level) is essential for reliable
62 flood risk assessment. There have been studies on regional or river basin scales (Allen et al., 2016; Ghosh &
63 Kar, 2018; Roy et al., 2021); however, those do not provide flood risk at a sub-basin scale in India. In addition,
64 the impact assessment of floods on transport infrastructure (rail and road infrastructure) still needs to be improved
65 in the country (Pathak et al., 2020; P. Singh et al., 2018). In addition, the role of dams and reservoirs in the flood
66 risk assessment should be addressed (Hirabayashi et al., 2013; Yamazaki et al., 2018). Dams and reservoirs
67 considerably influence streamflow variability and can attenuate flood peaks (Dang et al., 2019; Vu et al., 2022;
68 Zajac et al., 2017). In contrast, dam operations and decisions can also worsen the flood situation in the downstream
69 regions. For instance, recent flooding in Kerala and Chennai was partly attributed to reservoir operations (V.
70 Mishra & Shah, 2018). India has more than 5300 large dams regulating river flow (National Register of Large
71 Dams (NRLD), 2019), affecting ecosystems, natural resources, and livelihoods (Acreman, 2000). Reservoirs
72 impact flow regulation, magnitude, timing, and extent of flooding in the downstream regions. Therefore, flood
73 risk assessment without considering the role of reservoirs can be inappropriate in the basins that are highly affected
74 by the presence of dams.

75 We use the H08 (Hanasaki et al., 2018) global hydrological model combined with the CaMa-Flood (Yamazaki et
76 al., 2011) model for the sub-basin level flood risk assessment in India considering the role of reservoirs. The
77 CaMa-Flood model combined with the H08 model has been used for several river basins globally (Boulange et
78 al., 2021; C. M. R. Mateo et al., 2013). The CaMa-Flood model performs well in simulating flood dynamics

Deleted: (

Formatted: Font: 11 pt

Formatted: Font: 11 pt

Deleted: (

Formatted: Font: 11 pt

Deleted: ,

82 (Chaudhari and Pokhrel, 2022; H. Dang et al., 2022; Gaur & Gaur, 2018; Hirabayashi et al., 2013, 2021;
83 Yamazaki et al., 2018; Yang et al., 2019). The CaMa-Flood model takes runoff as input simulated from any
84 hydrological model and can simulate flood depth and inundation. In India, almost all the major rivers are
85 influenced by reservoirs (Lehner et al., 2011). Therefore, the major scientific questions that we address are: 1)
86 How does the flood risk vary at the sub-basin scale in India for the observed worst floods that occurred during the
87 1901-2020 period? 2) Which are the sub-basins where the presence of reservoirs considerably influences the flood
88 risk? To address these questions, we use long-term observations (1901-2020) from India Meteorological
89 Department (IMD) along with a hydrological modelling framework.

90 2. Data and Methods

91 2.1 Datasets

92 We used observed gridded precipitation (Pai et al., 2014) and daily maximum and minimum temperatures
93 (Srivastava et al., 2009) from India Meteorological Department (IMD). We obtained gridded daily precipitation
94 at 0.25° from IMD for the 1901-2020 period that was developed using station-based rainfall observations from
95 more than 6900 gauge stations (Pai et al., 2014). The gridded rainfall product has been widely used for
96 hydrological studies (Kushwaha et al., 2021; Shah & Mishra, 2016) and it captures the key features of the
97 summer monsoon variability and orographic rainfall over the western Ghats and foothills of the Himalayas. We
98 obtained daily 1° gridded maximum and minimum temperatures from IMD (Srivastava et al., 2009). The gridded
99 temperature dataset is developed using observations from 395 stations located across India. Bilinear interpolation
100 was used to convert the 1° gridded temperature to 0.25° resolution to make it consistent with the gridded
101 precipitation. For the regions outside India, we obtained observational meteorological datasets (rainfall and
102 temperature) at 0.25 degrees from Princeton University (Sheffield et al., 2006). Gridded datasets from Sheffield
103 et al. (2006) compare well against the IMD observations and have been used in hydrological applications in India
104 (Shah & Mishra, 2016).

105 Observed daily streamflow at gauge stations and reservoir live storage were obtained from India Water Resources
106 Information System (India-WRIS). We considered the influence of 51 major reservoirs located in different river
107 basins to examine the impact of reservoirs on floods using the CaMa-Flood model (Figure S1). The information
108 of dams was obtained from the National Register of Large Dams (NRLD) [Table S1]. We used the Global Surface
109 Water (GSW) extent to estimate flood occurrences at a monthly timescale (Pekel et al., 2016). Simulated flood
110 occurrences during the period of the GSW database (1985-2020) were used to validate the performance of the
111 hydrological model in simulating flood extent (Pekel et al., 2016). In addition, we obtained reported flood details
112 from the Emergency Events Database (EM-DAT, <http://www.emdat.be/>) and Dartmouth Flood Observatory
113 (DFO, <http://floodobservatory.colorado.edu/>). EM-DAT is developed by the Centre for Research on the
114 Epidemiology of Disasters (CRED), while the University of Colorado manages DFO. We used population data
115 from Global Human Settlement Layers (GHLS) to estimate flood exposure. Finally, we used roadway and railway
116 network data to assess the impact of floods on the infrastructure.

117 2.2 H08-CaMa-Flood combined model

Formatted: Font: 11 pt

Formatted: Font: 11 pt

Formatted: Font: 11 pt

Deleted: the

Deleted: occurrence

Formatted: Font colour: Auto

Deleted:).

Formatted: Font colour: Black

121 We used the H08 (Hanasaki et al., 2018) global hydrological model to simulate hydrological variables. The H08
122 is a distributed global water resources model comprising six sub-models: land surface hydrology, river routing,
123 reservoir operation, crop growth, environmental flow, and water abstraction. The model estimates baseflow using
124 a leaky bucket method, while runoff is calculated based on saturation excess non-linear flow (Hanasaki et al.,
125 2008). The H08 model can be run separately or combined with any hydrodynamic model to perform flow routing.
126 The H08 model uses precipitation, air temperature, short and longwave radiations, wind speed, surface pressure,
127 and specific humidity as input meteorological forcing. Soil parameters for the H08 model were obtained from
128 Harmonized World Soil Database (HWSD). We forced the H08 model with the input meteorological forcing at
129 0.25° spatial and daily temporal resolution. We combined the H08 land surface model with the CaMa-Flood
130 model. The CaMa-Flood model has been previously combined with the H08 model to obtain flood inundation
131 estimates (C. M. Mateo et al., 2014).

132 The CaMa-Flood (version 4.1) is a hydrodynamic model (Yamazaki et al., 2011), which simulates river-floodplain
133 dynamics (Yamazaki et al., 2013). The CaMa-Flood model has been extensively used for better performance in
134 simulating discharge and flood peaks (Zhao et al., 2017). The CaMa-Flood model considers the role of dams and
135 reservoirs for streamflow and flood inundation simulations (Chaudhari & Pokhrel, 2022; C. M. Mateo et al.,
136 2014; Pokhrel et al., 2018). We ran the CaMa-Flood model at a finer spatial resolution (0.1°) using the H08-
137 simulated runoff (0.25°) as input. We calibrated the combined model (H08 and CaMa-Flood) for India's eighteen
138 major river basins for at least one gauge station, each, considering the influence of 51 major dams. The gauge
139 stations were selected in the farthest downstream of the river basin based on the availability of observed
140 streamflow. The influence of reservoir operations was simulated using the CaMa-Flood model and evaluated
141 against the observed daily live reservoir storage.

142 We manually calibrated the H08 model by adjusting four parameters for each river basin, which include single-
143 layer soil depth, gamma, bulk transfer coefficient, and tau (Hanasaki et al., 2008). We evaluated the model
144 performance using the coefficient of determination (R^2) and Nash-Sutcliffe Efficiency (NSE) for daily streamflow
145 and reservoir live storage. In addition, we compared the simulated and satellite-based observed flood occurrences.
146 The satellite-based flood occurrence is calculated using the Global Surface Water (GSW) dataset (Pekel et al.,
147 2016), available for the 1984-2020 period. We forced the well-calibrated combined (H08 and CaMa-Flood)
148 models with observed meteorological forcing from India Meteorological Department (IMD) at 0.25° spatial
149 resolution to conduct simulations from 1901 to 2020. The H08 model simulated runoff is used in CaMa-Flood to
150 rout flood dynamics at six arc-minutes (0.1 degrees). We generated the flood depth maps for the historical worst
151 flood at the sub-basin level. The worst flood is based on the highest magnitude of river flow observed at the
152 subbasin outlet. The generated flood depths at 6 arc-minutes (0.1°) were further downscaled to 1 arc-minute
153 (~0.185 km) resolution using the downscaling module available within the CaMa-Flood.

154 We used C-ratio (Nilsson et al., 2005; Zajac et al., 2017) to assess the potential impact of dams along a river. The
155 C-ratio is an identifier calculated as the ratio of total maximum storage capacity of the upstream reservoirs to the
156 mean annual discharge at a gauge station in the downstream region (Nilsson et al., 2005; Zajac et al., 2017). We
157 calculated the C-ratio at the outlets of each sub-basins that are influenced by the presence of dams. A C-ratio of
158 less than 0.5 indicates that the sub-basin is minimally affected by the presence of dams. Further, to identify sub-

Formatted: Font: 11 pt

Deleted: ,

Deleted: estimate

Deleted: dam effect

Deleted: a reservoir's

Deleted: selected point along

Deleted: river

Deleted: lower (

Deleted:) C-ratio

Deleted: not considerably

168 basins susceptible to flood inundation resulting from dam operations, we multiplied the percentage of flooded
169 area in each sub-basin by its corresponding C-ratio. This enabled us to identify the sub-basins that experience
170 substantial flood inundation and are considerably impacted by the presence of reservoirs. Finally, we estimated
171 the exposed rail and road infrastructure affected by floods. The flooded area overlapped over the road and railway
172 network to estimate the network length affected by floods in a sub-basin. We considered the flooded area of the
173 observed worst flood. The subbasins with the highest rail and road infrastructure exposure to floods were
174 identified.

175 2.3 Risk assessment

176 We estimated flood risk using hazard, exposure, and vulnerability based on the common framework adopted by
177 the United Nations in the Global Assessment Reports of the United Nations Office for Disaster Risk Reduction
178 (UNISDR, 2011, 2013). A similar framework was used in previous studies for flood risk assessments (C. M. R.
179 Mateo et al., 2014; Tanoue, 2020; Winsemius et al., 2013). We multiplied the normalized values of hazard,
180 exposure, and vulnerability to estimate the risk as:

$$181 \quad \text{Risk} = \text{Vulnerability} * \text{Exposure} * \text{Hazard} \quad \dots \dots (1)$$

182 The flood risk assessment can help identify the hotspots and prioritize climate adaptation (de Moel et al., 2015).
183 Among the three components, vulnerability is a degree of damage to a particular object at flood risk with a
184 specified amount and present on a scale from 0 to 1. We obtained the vulnerability index for each district from
185 the “Climate Vulnerability Assessment for Adaptation Planning in India Using a Common Framework”, a report
186 developed by the Department of Science and Technology
187 (<https://dst.gov.in/sites/default/files/Full%20Report%20%281%29.pdf>). The vulnerability of each district is
188 calculated using 14 indicators, each with equal weights. The indicators capture both sensitivity and adaptive
189 capacity. We estimated the vulnerability index of each sub-basin by taking the spatial mean of the vulnerability
190 of the districts falling into the sub-basins. Exposure is termed as assets and population in a flood-exposed area
191 resulting in flood damage (Marchand et al., 2022). The population dataset is a critical component in performing
192 exposure estimation. The exposure is defined as the fraction of the population exposed to the flood extent (Smith
193 et al., 2019). We completed the flood exposure estimate using the Global Human Settlement Layers (GHSL)
194 population dataset (Joint Research Centre (JRC) et al., 2021), which is available at a resolution of 30 arc-seconds
195 for 1975, 1990, 2000, 2014 and 2015. We used the population data for the year 2015 throughout this study. We
196 rescaled the population data to 6 arc-minutes to make it consistent with the flooded area simulated from the
197 combined model. We estimated the hazard as the exceedance probability of a flooded area exceeding half of the
198 historical maximum flooded area in the last 50 years. We used normalized vulnerability, exposure, and hazard to
199 estimate the risk.

200 3. Results

201 3.1 Calibration and evaluation of hydrological models

202 We calibrated and evaluated the performance of the H08 and CaMa-Flood combined models against the observed
203 daily streamflow (Figure 1). Due to the unavailability of daily observed streamflow for the three transboundary
204 river basins (Indus, Ganga and Brahmaputra), we used observed monthly streamflow to calibrate the model. In

- Deleted: of
- Deleted: with their
- Deleted: , which was used
- Deleted: considerable
- Deleted: affected
- Deleted: The identified sub-basins are prone to flooding due to dam operations.

Deleted: Fig.

213 addition, we evaluated the model performance for daily live storage of the 51 reservoirs after the calibration
214 against the observed flow (Figure 1). The model exhibited good skills ($R^2 > 0.6$ and $NSE > 0.6$) for almost all the
215 river basins except Cauvery, East Coast, Northeast Coast, and Sabarmati. The model also performed well with
216 $NSE > 0.6$ for more than 80% of the selected reservoirs in simulating daily live storage for the selected
217 reservoirs. We estimated the bias and timing error in simulating peak discharge at all the selected gauge stations
218 (Figure S2). We calculated the bias in the model simulated annual maximum streamflow against the observed
219 annual maximum streamflow for the time periods for which observations are available. We excluded the
220 transboundary rivers (Ganga, Brahmaputra and Indus) as timing error (in days) could not be estimated due to the
221 unavailability of daily observed flow. While other gauge stations exhibited moderate bias, gauge stations in
222 Cauvery, Sabarmati, and Mahi rivers basins show a considerable dry bias. Contrary to several other stations where
223 the mean timing error was below two days, the Sabarmati river basin displayed a comparatively higher mean
224 timing error. The relatively poor performance of the model in these river basins can be attributed to the lack of
225 long-term observations as well as substantial human interventions that can affect the observed flow.

226 We compared model-simulated, and satellite-based observed flood occurrence for the 1984-2020 period (Figure
227 2). In addition, we compared the model-simulated flood events against Sentinel-1 SAR and MODIS satellite-
228 based imagery for a few flood events based on the satellite data availability (Figures. 3, S3, S4). We found that
229 the model simulated flood extent captures the satellite based flood extent. However, we note that the model
230 overestimated the flood extent in Ganga river basin and underestimated in Brahmaputra river basin, therefore,
231 showing a non-systematic bias. Moreover, a considerable difference in the flood extent based on the two satellite
232 datasets was observed, which highlights the observational uncertainty in the estimation of flood extent. In general,
233 the model exhibits satisfactory performance in simulating flood extent against the satellite-based observations.
234 However, the model overestimates flood extent in the Ganga basin, which could be attributed to the influence of
235 cloud contamination and dense vegetation cover on satellite-based flood estimates (Chaudhari & Pokhrel,
236 2022). On the other hand, the model underestimates the flood occurrence in the upstream region of the
237 Brahmaputra River. This could be due to limitations in model parameterization, as observed flow is limited in the
238 transboundary river basins. Despite the good performance against the observed streamflow, the simulated flood
239 extent has a considerable bias, which can be attributed to satellite-based flood extent mapping limitations and the
240 model's ability to capture the flood extent accurately. The model-simulated flood extent shows a good agreement
241 against the reported flood from EM-DAT and DFO databases (Figure S5). In addition, the simulated flood extent
242 also showed a good agreement with the reported flood in cities in the Brahmaputra and Ganga River basins. Given
243 the limitation in the streamflow and flood extent observations, the hydrological models perform satisfactorily and
244 can be used for the sub-basin level risk assessment.

Deleted: Fig.

Deleted: 55

Deleted: 5

Deleted: coast

Deleted: Pennar

Deleted: (

Deleted: >

Deleted: 5)

Deleted: In addition, we

Deleted: Fig. 2). The

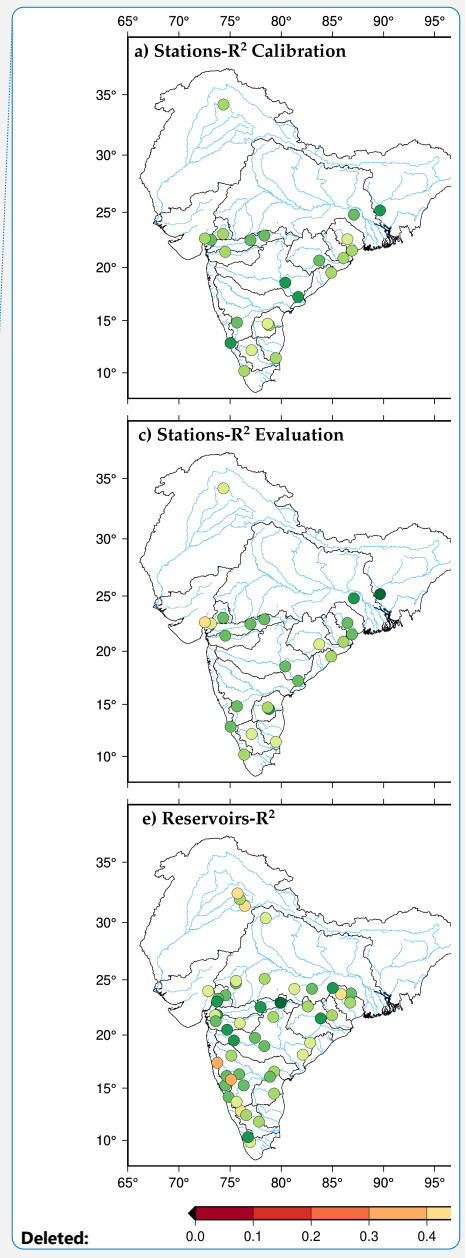
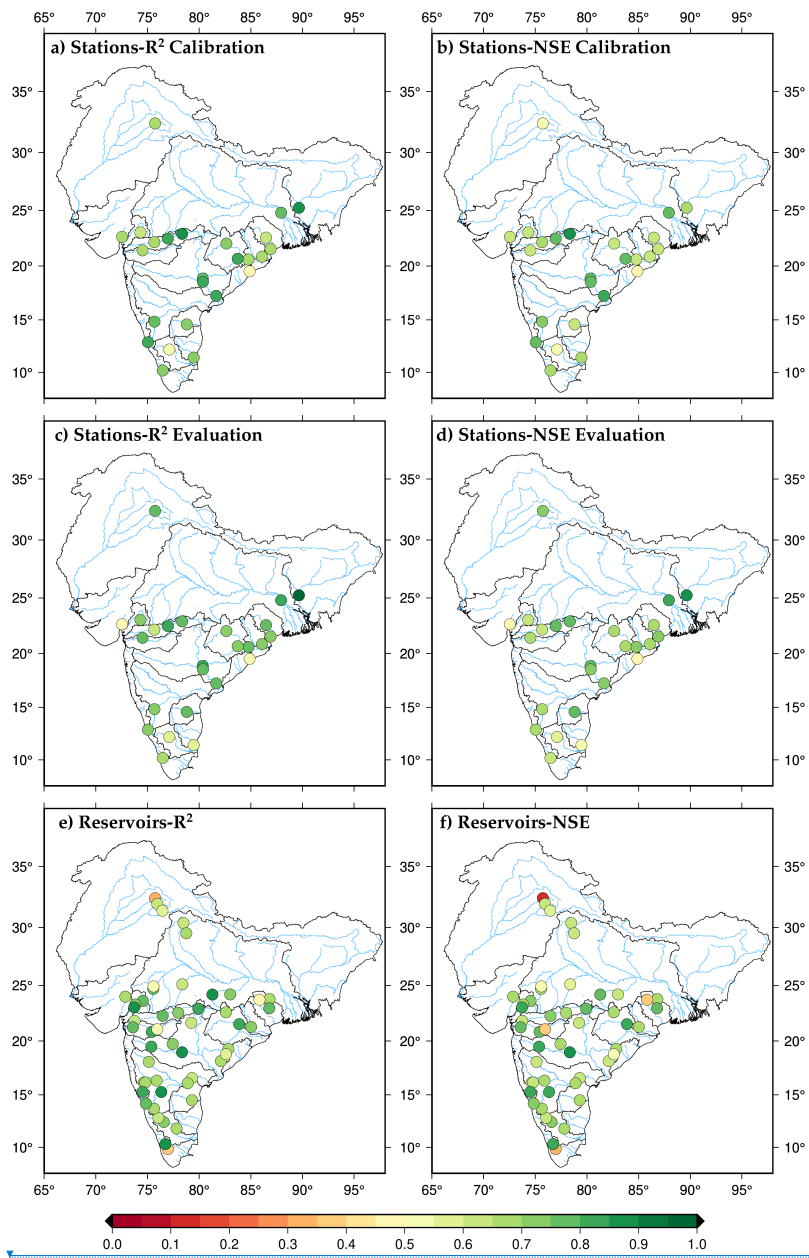
Deleted: the

Deleted: can

Deleted: due

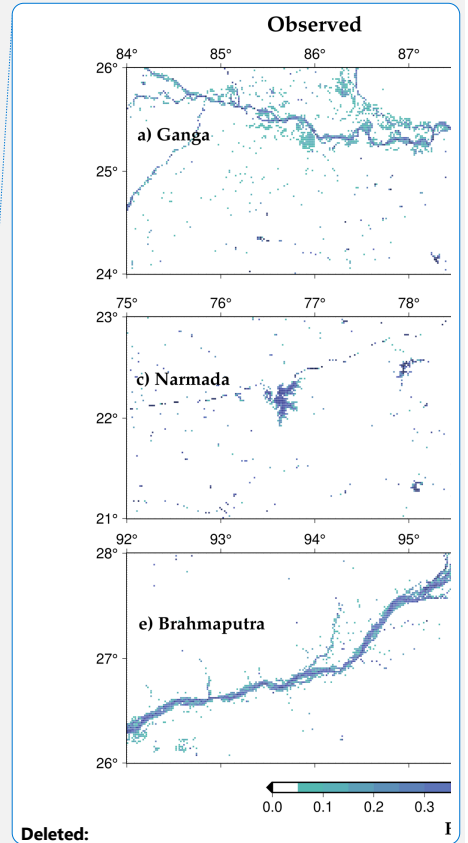
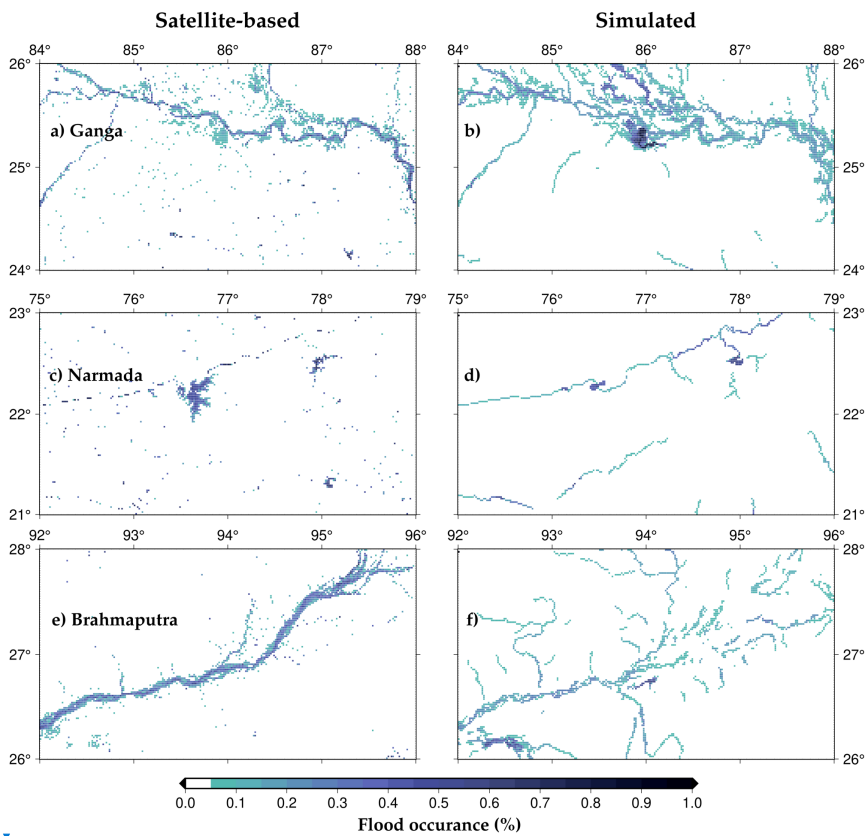
Formatted: Font: 11 pt

Deleted: Fig. S1



259

260 Figure 1: Calibration and evaluation of the combined model for daily river flow and reservoir storage at
 261 gauge stations and daily live storage of reservoirs

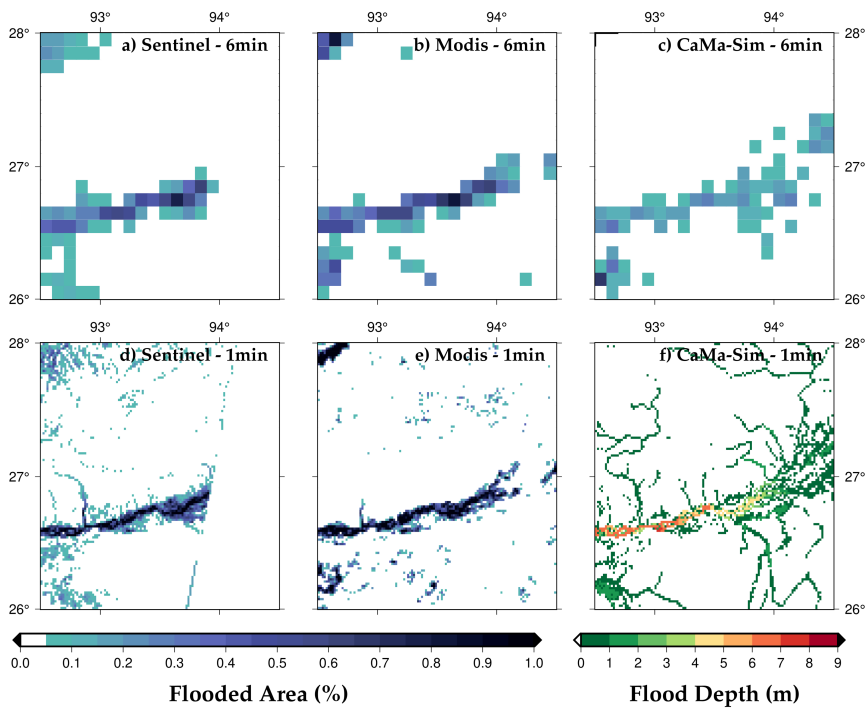


Deleted:

Deleted: observed

263

264 Figure 2: Simulated flood occurrences compared with satellite-based flood occurrence for different
 265 regions in Ganga, Narmada and Brahmaputra River basin.



268

269 **Figure 3: Simulated flood extent compared with Sentinel-1 SAR and MODIS satellite-based flood extent**
 270 **for the 2016 flood event in the Brahmaputra river**

271 **3.2 Estimation of the observed flood extent**

272 Next, we reconstructed the flood inundation for the observed worst flood for each sub-basin for the 1901-2020
 273 period in India. The inundation extent for the worst flood can help us identify the sub-basin with higher flood risk.
 274 We estimated flood depth and inundated area for each sub-basin for the worst flood during the last 120 years
 275 (Figure 4). In addition, we identified the occurrence of the worst flood at the sub-basin level during the 1901-2020
 276 period. We highlighted ten sub-basins that experienced the highest fractional area affected by the worst flood.
 277 Sub-basins in the Ganga and Brahmaputra rivers are among the most highly influenced by the worst flood. For
 278 instance, Ghaghra, Kosi, Bhagirathi, Gandak, Gomti, lower Sabarmati, upper Yamuna, Ramganga, and Baitarani
 279 sub-basins had the highest fractional area affected by the worst flood during 1901-2020 (Figure 4). The fractional
 280 area of sub-basins in the semi-arid western India is less affected compared to those located in the Ganga basin.
 281 For example, the lower Sabarmati sub-basin of the Sabarmati River basin is among the sub-basins that are highly
 282 influenced by the observed worst flood. We also find that the worst flood in the same year did not affect all the
 283 sub-basins within a river basin (Figure S6). For instance, all the highly influenced sub-basins experienced the
 284 worst flood in different years in the Ganga basin (Figure 4). Most of the top flood-affected sub-basins experienced
 285 floods during August-September in the summer monsoon season. Overall, the flood extent due to the worst flood

Deleted: 3

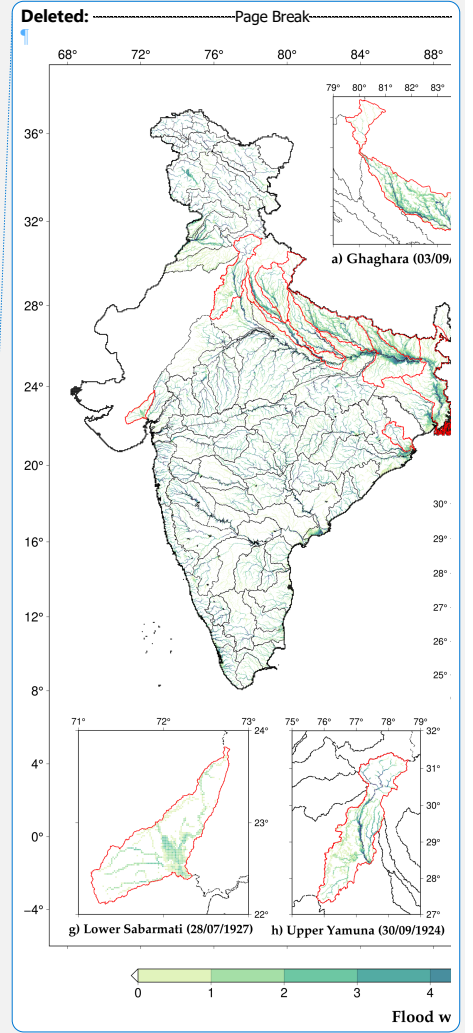
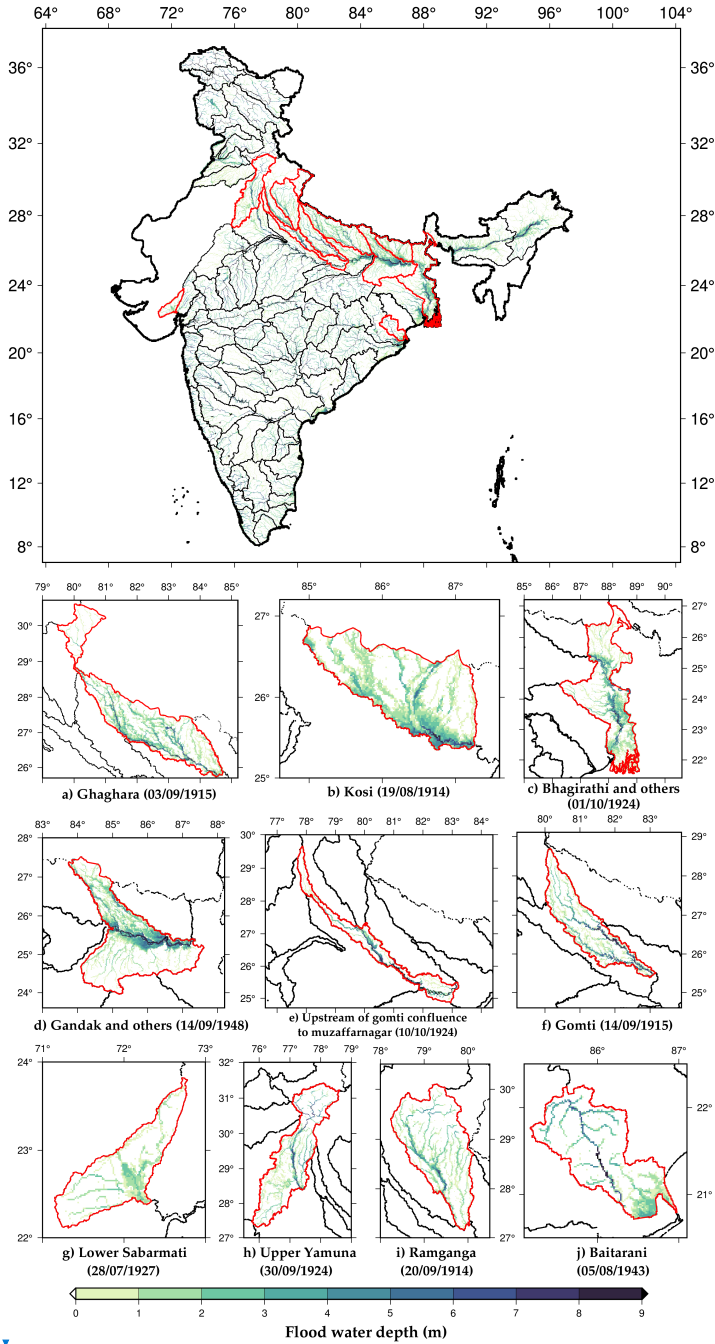
Deleted: Fig. 3

Deleted: .

Deleted: Fig. 3

290 is substantially greater in the sub-basins of the Ganga and Brahmaputra river basins compared to other basins in
291 India (Figure 4). Ganga river basin also has the highest population density among all the basins in the Indian sub-
292 continent, which makes it vulnerable for the flood risk.

Deleted: Fig. 3



298 **Figure 4: Flood depth map for the observed worst flood for each sub-basins, highlighting the sub-basins**
299 **with maximum flood inundated area (%) (a) Ghaghara – Ganga River basin (b) Kosi – Ganga River basin**
300 **(c) Bhagirathi and others – Ganga River basin (d) Gandak and others – Ganga River basin (e) Upstream**
301 **of Gomti confluence to Muzaffarnagar – Ganga River basin (f) Gomti – Ganga River basin (g) Lower**
302 **Sabarmati – Sabarmati River basin (h) Upper Yamuna – Ganga River basin (i) Ramganga – Ganga River**
303 **basin (j) Baitarani – Brahmani River basin**

Deleted: 3

304 Next, we examined the precipitation, streamflow, and flood-affected area (%) for the ten sub-basins that had the
305 highest fractional flood affected area for the worst flood during 1901-2020 (Figure 5). As floods mostly occur
306 during the summer monsoon season in India (V. Mishra et al., 2022; Nanditha & Mishra, 2021), we examined
307 the temporal variability of precipitation, and streamflow during the monsoon season of the worst flood year.
308 Nanditha and Mishra (2022) reported that multi-day precipitation is India's most robust driver of floods. Moreover,
309 extreme precipitation and wet-antecedent conditions trigger floods in India (Nanditha & Mishra, 2022). We
310 find that the Ghaghara sub-basin of the Ganga river experienced the worst flood in September 1915, affecting
311 more than 10,000 km² area of the sub-basin. A multi-day rainfall in late August and early September (1915) caused
312 the worst flood in the basin. The Kosi sub-basin of the Ganga river experienced the worst flood in August 1914,
313 which affected more than 5000 km² of the basin (Figure 5). Similarly, Bhagirathi and other sub-basins in the
314 Ganga river basin were affected by the worst flood in late September 1924, which inundated more than 12000
315 km² of the sub-basin. Similarly, Gandak and Gomti river basins experienced the worst floods in 1948 and 1915,
316 respectively. Our results agree with the information presented in previous studies (Agarwal & Narain, 1991;
317 Fredrick, 2017; Joshi, 2014; D. K. Mishra, 2015; A. Singh et al., 2021). We find that most of the sub-basins
318 of the Ganga river basin are prone to large extents of flood inundation. Moreover, the worst floods in most sub-
319 basins were caused by multi-day precipitation, a prominent driver of floods in the Indian sub-continental river
320 basins (Figure 5).

Deleted: Fig. 4

Deleted: (

Formatted: Font: 11 pt

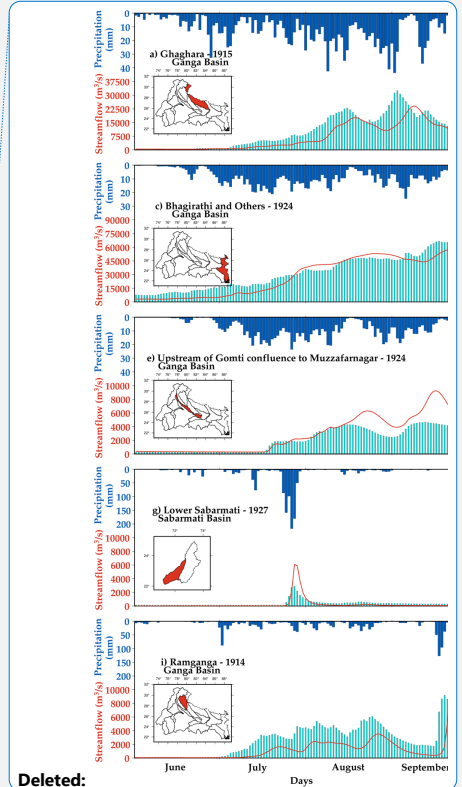
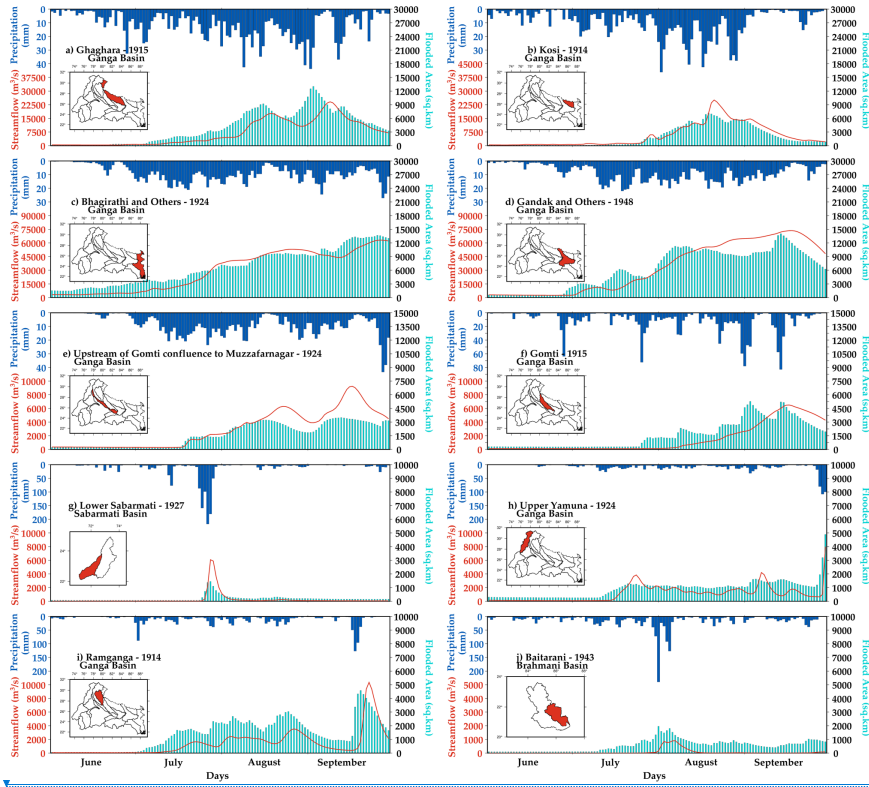
Formatted: Font: 11 pt

Deleted: 2014

Deleted: Fig 4

Moved (insertion) [1]

Deleted: Fig. 4



Deleted:

Deleted: 4

Deleted: 5a

Deleted: 5b

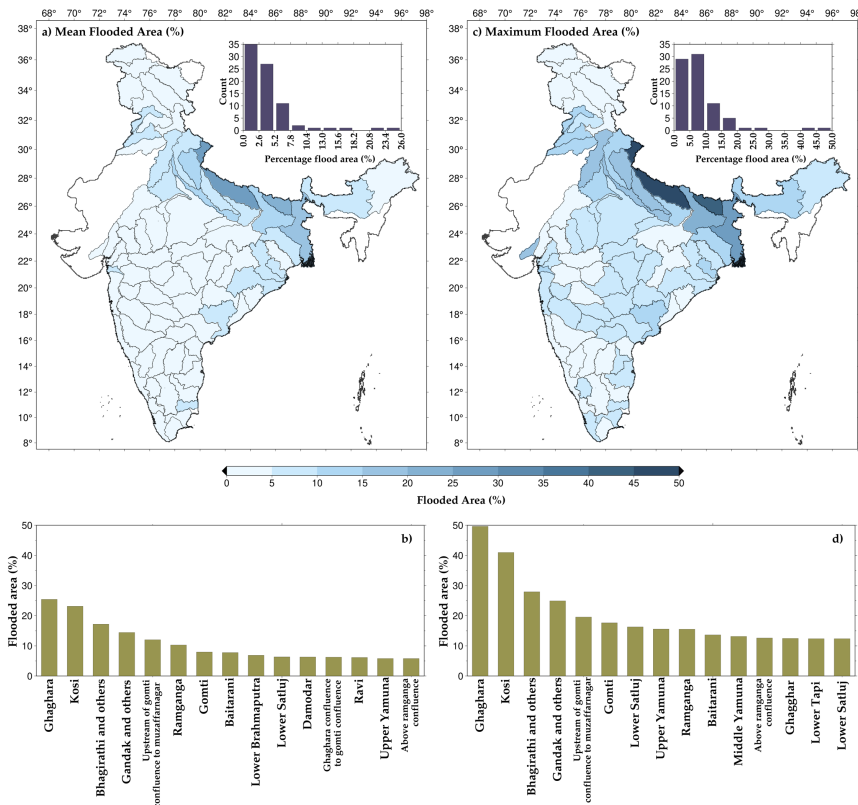
327

328 **Figure 5:** Daily upstream precipitation (mm, blue), the H08 model simulated streamflow (red) at the sub-
 329 basin outlet (m³/s), and flooded area (km², green) for the summer monsoon (June-September) period of
 330 the corresponding worst flood year. (a) Ghaghara - Ganga River basin (b) Kosi - Ganga River basin (c)
 331 Bhagirathi and others - Ganga River basin (d) Gandak and others - Ganga River basin (e) Upstream of
 332 Gomti confluence to Muzaffarnagar - Ganga River basin (f) Gomti - Ganga River basin (g) Lower
 333 Sabarmati - Sabarmati River basin (h) Upper Yamuna - Ganga River basin (i) Ramganga - Ganga River
 334 basin (j) Baitarani - Brahmani River basin

335 To further examine the flood-affected area at the sub-basin level, we estimated the mean annual maximum flooded
 336 area (Figure 6a) and historical maximum flooded area using the H08-CaMa flood models (Figure 6b). Most of the
 337 highly flooded sub-basins are in the Ganga River basin. While the mean annual maximum flooded area for the
 338 top flood-affected sub-basins ranged between 10 to 15%, their maximum flooded area varied between 30 to 40%.
 339 Other than sub-basins from the Ganga river basin, Baitarani, lower Tapi, lower Godavari, Brahmani, and lower
 340 Mahanadi also showed a considerable mean flooded area during the 1901-1920 period. In the case of the maximum
 341 flooded area, Gandak, Kosi, and Ghaghara confluence to Gomti confluence sub-basins exhibited more than 20%
 342 flooded area. Sub-basins from the other river basins, such as lower Tapi, lower Narmada, Baitarani, and lower

347 Satluj, are in the top fifteen sub-basins with the highest flooded area. The sub-basins in the Ganga and
 348 Brahmaputra rivers are the most flood-affected. Moreover, the Ganga and Brahmaputra rivers experience the
 349 highest floods among all the river basins (Mohanty et al., 2020; Mohapatra & Singh, 2003).

Formatted: Font: 11 pt



350
 351 **Figure 6:** (a) Mean of annual maximum flooded area (percentage) between 1901-2020 and the overall
 352 distribution (b) highlighting the top fifteen sub-basin. (c) Historical maximum flooded area (percentage)
 353 and the overall distribution (d) highlighting the top fifteen sub-basin.

Deleted:

Deleted: 5

354 **3.3 Influence of reservoirs on flood extent**

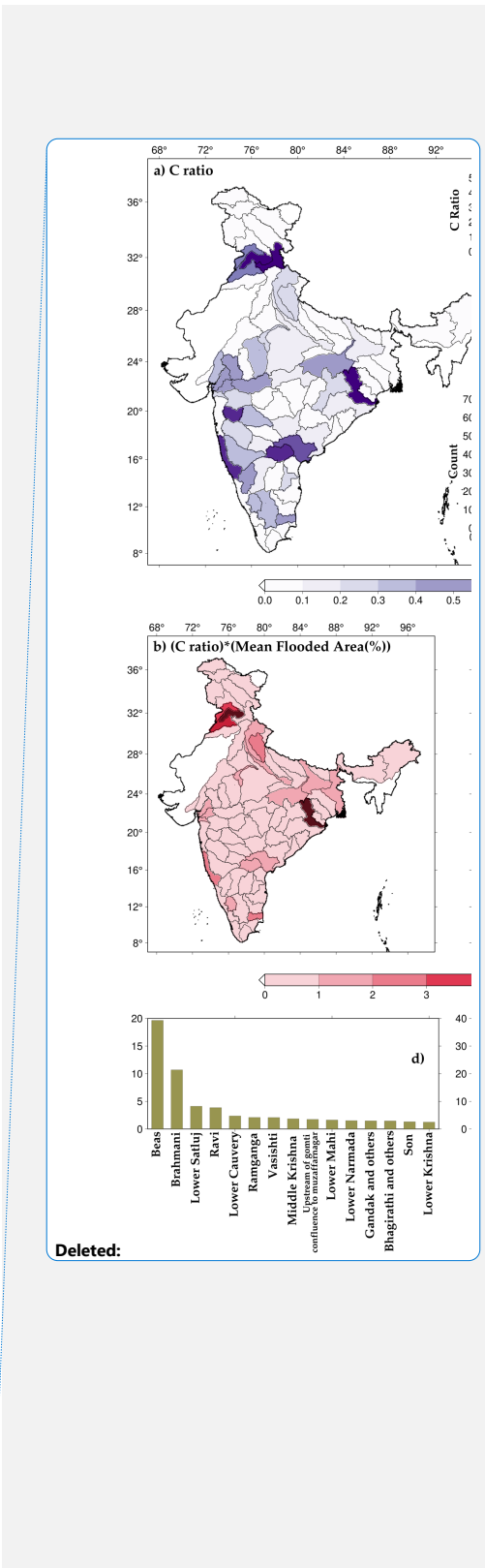
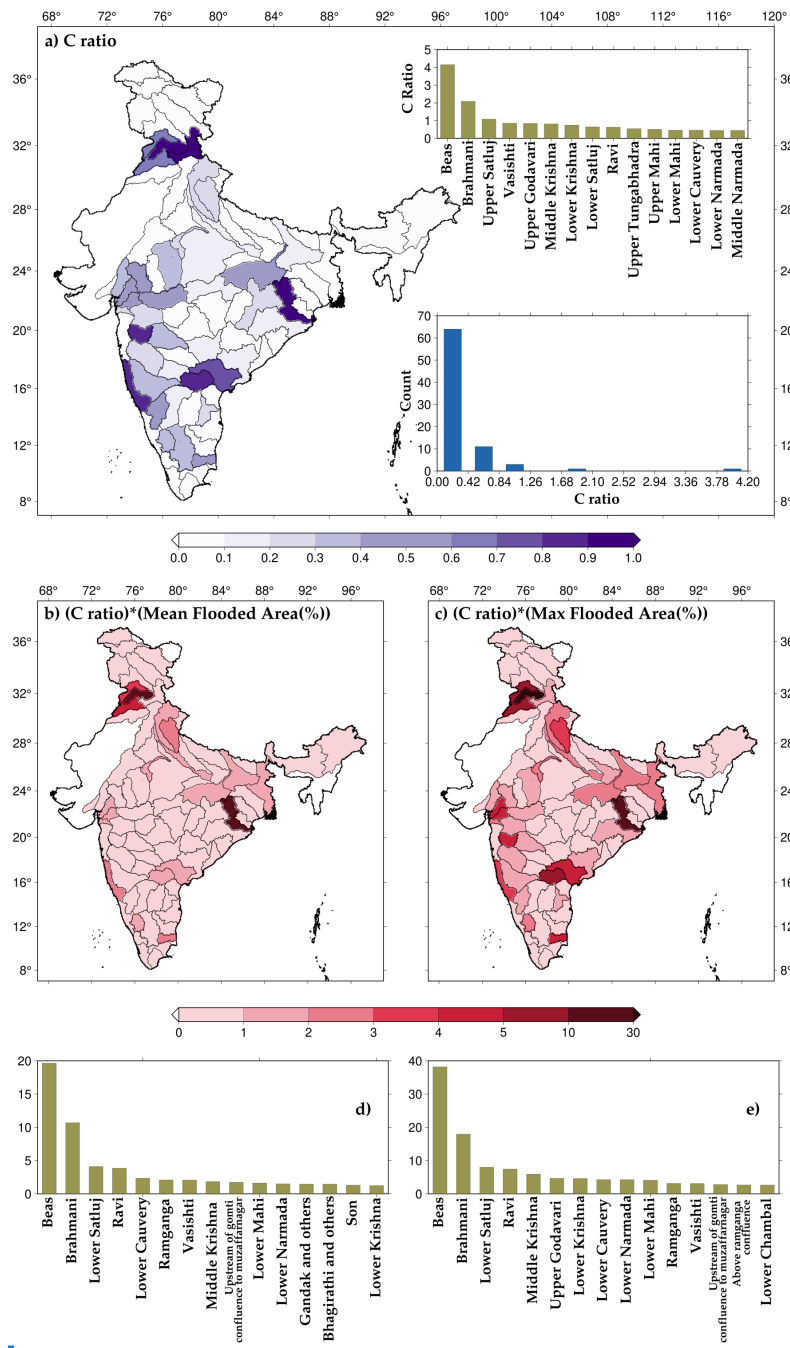
355 We selected and considered 51 major reservoirs to examine their influence on flood risk based on the availability
 356 of the observed storage data. We estimated C-ratio for each sub-basin considering the river flow at the outlet to
 357 investigate the impact of reservoirs on streamflow. C-ratio can vary between zero to infinity, and higher values
 358 indicate the prominent effect of dams on river flow. We identified sub-basins with a greater influence on dams
 359 based on the C-ratio. We find that Beas, Brahmani, upper Satluj, Upper Godavari, Middle and Lower Krishna,
 360 and Vashishti are among the most influenced by the dams. Beas sub-basin has the highest C-ratio (4.16) among

363 all the sub-basin in the Indian sub-continent (Figure 7a). Out of the 80 sub-basins, only eleven have C-ratio greater
364 than 0.5. 64 out of 80 sub-basins have a C-ratio between zero to 0.42 (Figure 7a). We considered only 51 major
365 reservoirs in our analysis. However, there are several major and minor dams for which observed data is
366 unavailable. Therefore, the influence of reservoirs based on the C-ratio might need to be considered. However,
367 our analysis indicates that dams in a few sub-basins can significantly alter the river flow and flood risk. For
368 instance, dams effectively alter extreme flow's timing, duration, and frequency (Mittal et al., 2016). C-ratio alone
369 may not effectively capture the influence of dams on floods; therefore, we multiplied the fractional area affected
370 by floods and the C-ratio for each sub-basins. For instance, if a sub-basin is considerably affected by dams and
371 has a large flood extent, the value of the multiplied ratio will be higher. The multiplier ratio can effectively identify
372 the sub-basins with high flood-affected areas and flow regulated by the reservoirs. We find that Beas, Brahmani,
373 Ravi, and Lower Satluj are among the highly influenced by floods and the presence of reservoirs. Overall, the
374 sub-basins with higher C ratio and the highest flood-affected area are across the Indian subcontinent. Central India
375 has sub-basins that are relatively less affected by floods and the presence of dams.

Deleted: 6a

Deleted: 6a

Deleted: c



381 **Figure 7: (a) Sub-basin wise C-ratio, top fifteen sub-basins and distribution of sub-basins based on C-ratio**
382 **values (b) Mean of annual maximum flooded area (percentage) multiplied with C-ratio (d) highlighting top**
383 **15 sub-basins (c) Historical maximum flooded area (percentage) multiplied with C-ratio (e) highlighting**
384 **top 15 sub-basins.**

Deleted: 6

385 3.4 Sub-basin level flood risk assessment

386 Next, we identified the roads (national highways) and railway exposure to riverine floods for each subbasin.
387 Climate change will adversely affect rail and road networks (Hooper & Chapman, 2012; Padhra, 2022). A
388 considerable length of roads is affected due to surface flooding resulting from high-intensity rain (Koks et al.,
389 2019). Therefore, we examined the impact of floods on rail and road infrastructure in India. We estimated the
390 length of the road and railway network potentially affected by the worst flood that occurred during 1901-2020.
391 We overlapped the road and rail network over the flooded area and estimated the network length exposed to floods
392 (Figures 8a-b). The estimated length for each sub-basin was normalized between zero and one (Figures 8c-d). We
393 find that the road network can be the most affected by the floods in the Gandak, Kosi and Ghaghara confluence
394 to Gomti confluence in the Ganga river basin. On the other hand, a considerable part of the rail network can be
395 affected by floods in Son, Kosi, and Upper Yamuna subbasins. Moreover, in Bhagirathi and Gandak river basins,
396 more than 50 km of road network falls in the flood-prone regions (Figure 8e). There are ten sub-basins in which
397 more than 20 km of road network falls in flood-prone areas of India. Similarly, over 20 km of the rail network is
398 in the flood-affected areas of the six sub-basins (Upper Yamuna, Son, Kosi, Brahmani) [Figure 8f].

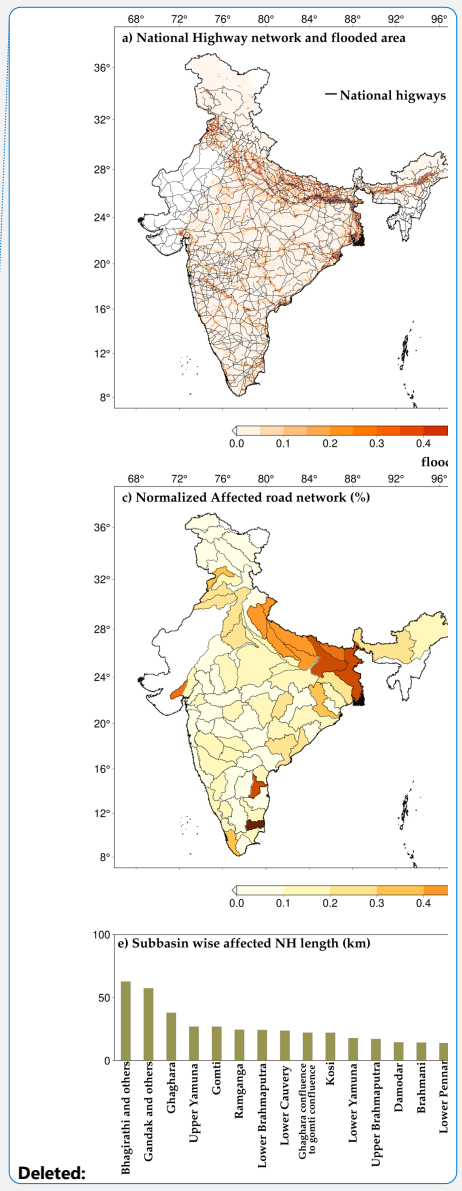
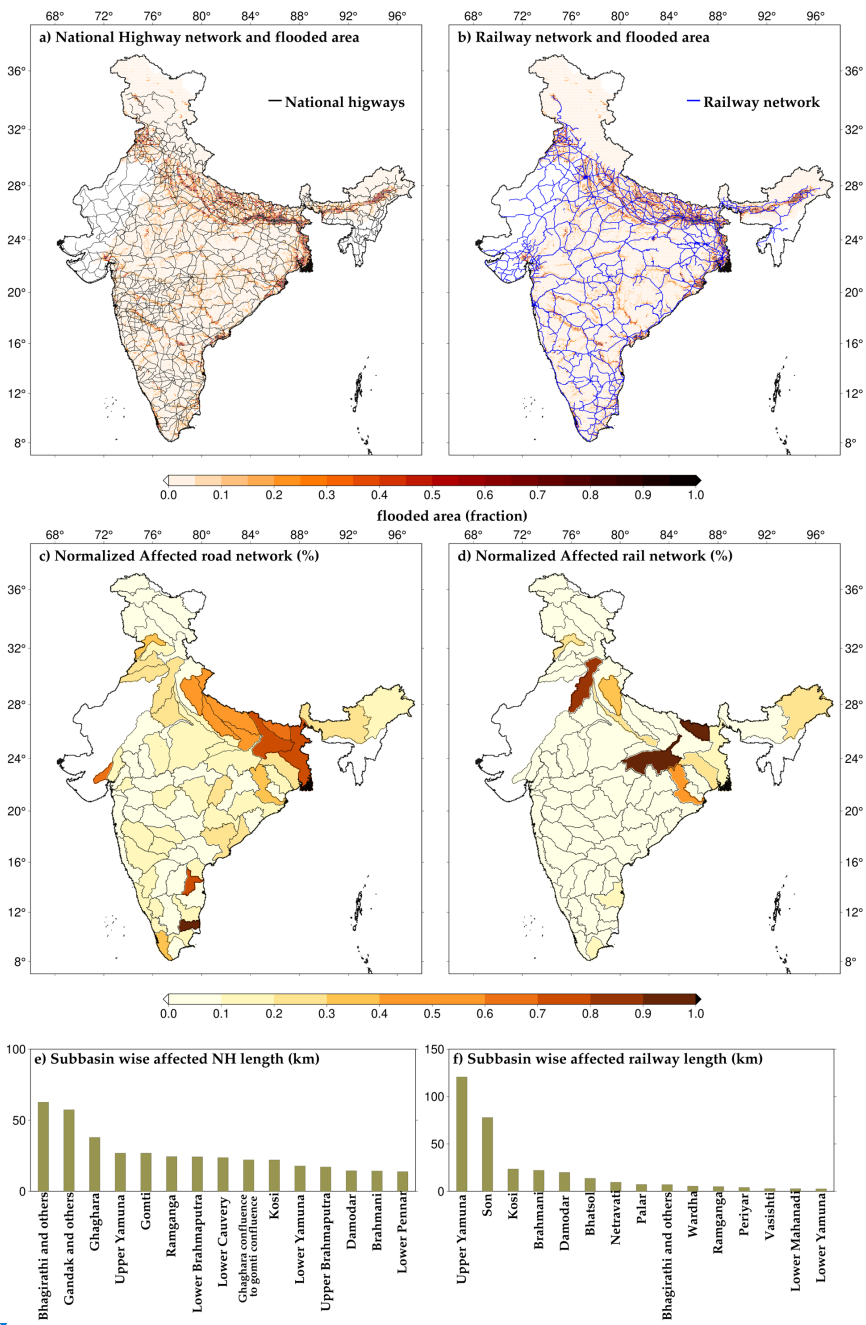
Formatted: Font: 11 pt

Deleted: Figure 7a

Deleted: Figure 7c

Deleted: 7e

Deleted: 7f



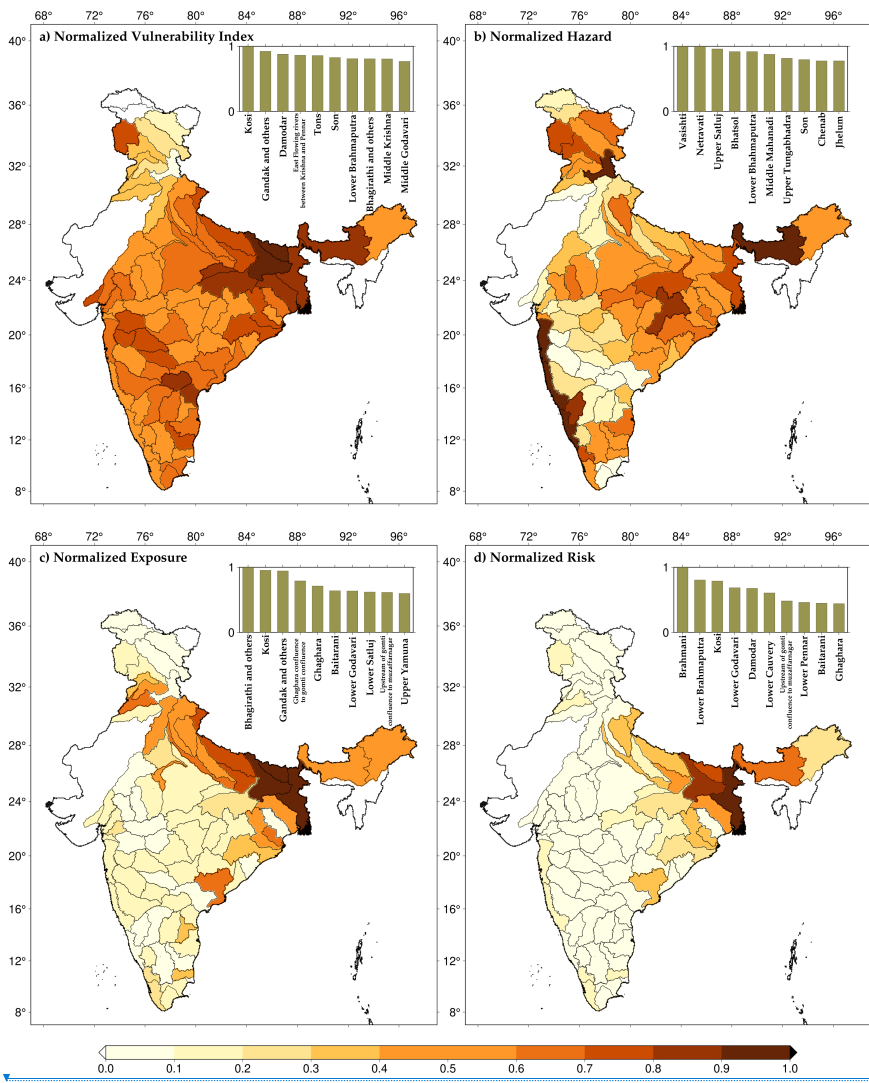
406 **Figure 8: Flood impacts on roads and railways infrastructure. (a-b) National Highways network and**
407 **Railway network overlapped over the flooded area in worst flood cases, (c-d) subbasin wise normalised**
408 **flood affected road and railway network (percentage), (e-f) top 15 subbasins with most affected national**
409 **highways and railway length (km).**

Deleted: 7

410 Finally, we estimated sub-basin level flood risk using normalized vulnerability, hazard, and exposure (Figure 9).
411 Vulnerability for each sub-basin in India was assessed using the national vulnerability assessment data available
412 at the district level. We estimated hazard probability considering 50% of the inundated area for the worst flood as
413 a benchmark. The likelihood of flood inundated areas in a sub-basin exceeding the benchmark was used in the
414 risk assessment. Similarly, we used the worst flood extent and gridded population data to estimate flood exposure.
415 The sub-basins in north-central India have a relatively higher vulnerability calculated using the socio-economic
416 indicators. The vulnerability is relatively lower in north India and the Western Ghats. Kosi, Gandak, and Damodar
417 sub-basins have the highest vulnerability. We find that hazard probability is higher in the sub-basins of
418 Brahmaputra, rivers in the western Ghats, and a few sub-basins of the Indus river basin (Figure 9b). For instance,
419 upper Satluj, Chenab, and Jhelum sub-basins of the Indus river have higher hazard probability. Other than the
420 Western Ghats, most sub-basins in Peninsular India have relatively lesser hazard probability. Exposure, which
421 represents the fraction of the population affected by flood under the worst flood scenario, is higher in the Indo-
422 Gangetic Plain. Apart from the sub-basins of the Ganga River basin, the lower Brahmaputra, lower Godavari, and
423 Baitarani sub-basin show higher exposure. Therefore, Ganga and Brahmaputra Rivers basins are the highest flood-
424 prone river basins and have high flood exposure. Rentschler et al. (2022) also reported that the highest population
425 exposure due to floods is in Uttar Pradesh, Bihar, and West Bengal, which is part of the Ganga river basin.

Deleted: 8

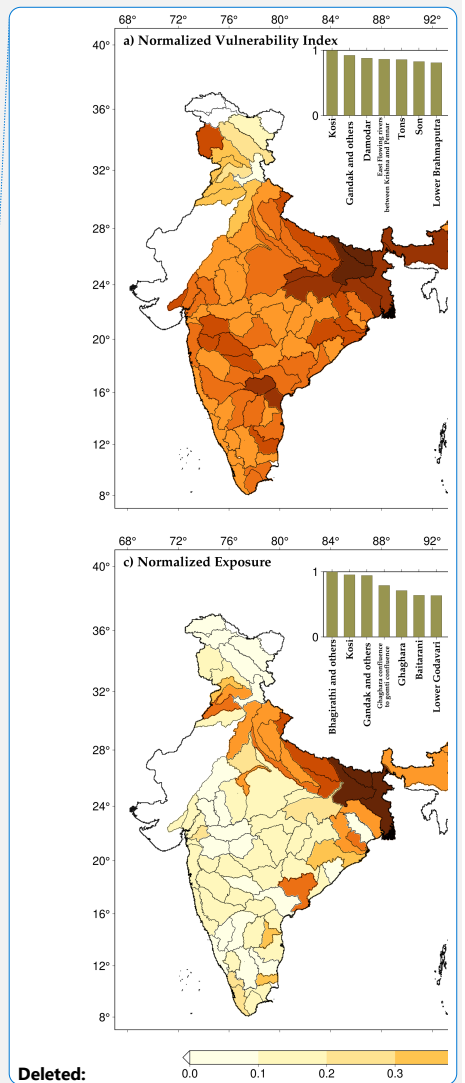
Deleted: Fig. 8b



429

430 **Figure 9:** Sub-basin level (a) Normalized vulnerability index (b) Normalized hazard (c) Normalized
 431 exposure (d) Normalized risk. The top 10 sub-basins are highlighted as bars in panels inside the figures.

432 We estimated the flood risk for each sub-basin, a collective representation of vulnerability, hazard, and exposure.
 433 As expected, the flood risk is higher in the Ganga and Brahmaputra river basins compared to other parts of the
 434 country. The higher flood risk in these basins can be attributed to higher vulnerability, hazard probability, and
 435 exposure. For instance, Bhagirathi, Gandak, Kosi, lower Brahmaputra, and Ghaghra are the sub-basins with the



Deleted:

Deleted: 8

438 highest flood risk in India (Figure 9d). Despite the higher hazard probability in the sub-basins of the Indus and
439 west coast river basins, the overall flood-risk is considerably lower than the sub-basins of the Ganga and
440 Brahmaputra river basins primarily due to less vulnerability and exposure. Our results show that flood risk in
441 some of the sub-basins of the Ganga and Brahmaputra river basins can be reduced by reducing the vulnerability.

Deleted: Fig. 8d

442 4. Discussion and conclusions

443 Flood risk mapping is essential for risk reduction and developing mitigation measures. The flood risk will likely
444 increase due to increased hazard probability and exposure (Ali et al., 2019). Hirabayashi et al. (2013) showed that
445 a warmer climate would increase the risk of floods on a global scale. In India also, floods are [expected to become](#)
446 more likely under warming climate. For instance, Ali et al. (2019) reported that multi-day floods are projected to
447 rise faster than single-day flood events. The projected rise in the flood frequency in India can be attributed to
448 increased extreme precipitation under warming climate (Mukherjee et al., 2018). Observational studies have also
449 concluded that there has been a considerable rise in extreme precipitation in India during the summer monsoon
450 season (Roxy et al., 2017), which is linked to warming climate. While the warming climate is directly linked to
451 the increased frequency of extreme precipitation, its association with riverine floods is not straightforward. For
452 instance, [Nanditha & Mishra \(2021, 2022\)](#) reported that multi-day precipitation on the wet antecedent condition
453 is the most favourable conditions for riverine floods in India.

Deleted: ..

454 While mapping the flood risk at appropriate spatial resolution is complex and challenging, it is vital for disaster
455 risk reduction. Flood inundation mapping that provides the spatial extent of flooding is crucial as the first
456 responders use it during a flood emergency (Apel et al., 2009). There are several approaches to mapping flood
457 inundation (Teng et al., 2017). We used hydrodynamic modelling to develop long-term flood inundation maps for
458 the Indian sub-basins. Creating [high-resolution flood inundation maps based on hydrodynamic modelling](#) is
459 computationally expensive (Dottori et al., 2016) [for a large domain like India](#). In addition, higher-resolution flood
460 risk mapping that can be used at the local scale for decision-making requires accurate terrain information and river
461 cross-section datasets that are not available. [For instance, freely available digital elevation models \(DEM\) can be](#)
462 [too coarse to resolve the flood inundation and depth variability at a local scale \(Cook & Merwade, 2009; Dey](#)
463 [et al., 2022\)](#). The uncertainties within hydrologic outputs can primarily arise due to inaccuracies in both input
464 [data and model parameterization \(Poulin et al., 2011\)](#). Inaccuracies in input meteorological data may stem from
465 [disparate sources, leading to errors in spatial and temporal interpolation \(Brown & Heuvelink, 2005\)](#). Similarly,
466 [model parameterization errors, which involve assigning values to parameters governing diverse hydrological](#)
467 [processes, can emerge during the calibration process \(Laiolo et al., 2015\)](#). Moreover, there are uncertainties
468 [originating from utilizing long-term flood occurrence data to assess flood mapping capabilities. Our modelling](#)
469 [framework that considers the influence of reservoirs provides sub-basin scale flood inundation extent as our aim](#)
470 [was to provide a long-term assessment of flood extent in at the country scale. Additionally, downscaling of flood](#)
471 [depths introduces biases as coarse-scale information is translated to the local scale \(He et al., 2021\), which might](#)
472 [have considerable deviations from the actual observed flood extent](#). Given these limitations, our findings provide
473 valuable information based on the long-term record developed using model simulations that can be used for the
474 regional scale policy development for flood mitigation. Cloud cover during the summer monsoon, when most
475 floods occur in India (Nanditha et al., 2022), hinders the utility of satellite data for flood inundation mapping. We

Deleted: (

Formatted: Font: 11 pt

Deleted: ,

Formatted: Font: 11 pt

Deleted: two

Deleted: higher

482 calibrated and evaluated our H08-CaMa flood modelling framework using the observed flow, reservoir storage,
483 and satellite-based inundation. However, all these datasets available from the in-situ network or satellites are
484 prone to errors and uncertainty (Di Baldassarre & Montanari, 2009; Stephens et al., 2012; Teng et al.,
485 2017). We used C-ratio as an indicator to quantify the influence of dams on streamflow. However, C-ratio may
486 not fully capture the complexities and variations in the impacts of reservoir operations. Furthermore, in case of
487 run-of-the-river (RoR) dams, the C-ratio may over-estimate the downstream hydrological impacts. Therefore, C-
488 ratio may not solely capture the downstream hydrological effects resulting from dams. Nevertheless, it provides
489 preliminary information on the potential dam influence on the downstream flow.

Formatted: Font: 11 pt

490 India has implemented several flood risk mitigation measures at multiple government levels. The construction of
491 embankments along rivers is a common flood risk mitigation measure in India. These embankments help contain
492 the floodwaters within the river channels and protect nearby areas from inundation (NDMA, 2016). The CWC in
493 India operates a network of flood forecasting stations that collect real-time data on rainfall and water levels to
494 forecast floods and issue warnings to vulnerable communities. Notwithstanding the considerable investments and
495 flood-control measures, India has witnessed substantial mortality, human migration, and economic loss. Flood
496 mortality has increased mainly because of increased frequency, not necessarily due to increased flood intensity
497 (Hu et al., 2018). About 3% of the total geographical area of India is affected by floods every year that cause
498 damage to agriculture and infrastructure. The top ten floods that occurred during 1985-2015 caused the mortality
499 of more than 1000 people while more than 35 million people were displaced due to floods between 2000-2004
500 (Dartmouth Flood Observatory). The recent riverine floods in Uttarakhand and Kerala highlighted the growing
501 flood risk in India, which warrants the need for flood mitigation. The recent flood in August 2022 in Pakistan
502 caused an estimated loss of \$30 billion. Both structural and non-structural measures are required for flood
503 mitigation (Nanditha & Mishra, 2021). Our risk assessment provides policy implications towards reducing
504 vulnerability to reduce the flood risk. Moreover, a sub-basin level ensemble forecast is needed to be used for early
505 flood warnings in the sub-basins with higher flood risk.

Formatted: Font: 11 pt

506 Based on our findings, the following conclusions can be made:

- 507 • The coupled hydrological and hydrodynamic modelling framework based on the H08-CaMa Flood model
508 was used to estimate the flood risk assessment in India. The hydrological modelling framework
509 performed well against the observed flow, reservoir storage, and satellite-based flood inundation. The
510 role of 51 major reservoirs was considered in flood risk assessment based on the long-term simulations
511 for the 1901-2020 period.
- 512 • The sub-basins in the Ganga and Brahmaputra river basins experienced the most significant flood extent
513 during the worst flood in 1901-2020. Similarly, the mean annual maximum flood extent is higher for the
514 sub-basins in the two major transboundary river basins (e.g., Ganga and Brahmaputra). The worst flood
515 affected different sub-basins on the two main flood-affected river basins in different years. Major floods
516 in the flood-prone sub-basins of the Ganga and Brahmaputra basins occur during the summer monsoon
517 season, especially during the August-September period.
- 518 • The sub-basins with a more prominent influence of dams based on the C-ratio were identified. Beas,
519 Brahmani, upper Satluj, Upper Godavari, Middle and Lower Krishna, and Vashishti sub-basins are

520 among the most influenced by the dams. Moreover, Beas, Brahmani, Ravi, and Lower Satluj are among
521 the most affected by floods and the presence of reservoirs.

- 522 • Flood risk is higher in the Ganga and Brahmaputra river basins compared to other parts of the country.
523 The higher flood risk in the two transboundary river basins can be attributed to higher vulnerability,
524 hazard probability, and exposure. Bhagirathi, Gandak, Kosi, lower Brahmaputra, and Ghaghra are India's
525 sub-basins with the highest flood risk.

526 **Data availability:** All the datasets used in this study can be obtained from the corresponding author.

527 **Competing interest:** Authors declare no competing interest.

528 **Author contributions:** [VM designed the study. UV conducted the analysis and wrote the first draft. All the](#)
529 [authors contributed in the writing and discussion.](#)

530 **Acknowledgement:** The work was supported by the Monsoon Mission, Ministry of Earth Sciences. The
531 authors acknowledge the data availability from India Meteorological Department (IMD) and India-
532 WRIS. We acknowledge the database availability from EM-DAT: <http://www.emdat.be/>, DFO:
533 <http://floodobservatory.colorado.edu>, population data from GHSL:
534 <https://sedac.ciesin.columbia.edu/data/set/ghsl-population-built-up-estimates-degree-urban-smod>,
535 vulnerability assessment data from DST: [HYPERLINK](#)
536 "<https://dst.gov.in/sites/default/files/Full%20Report%20%281%29.pdf>"<https://dst.gov.in/sites>
537 </default/files/Full%20Report%20%281%29>

Formatted: Left, None, Indent: Left: 0.85 cm, Hanging: 0.85 cm, Space Before: 0 pt, After: 10 pt, Line spacing: Multiple 1.15 li, Don't keep with next, Don't keep lines together, Don't hyphenate, Don't adjust space between Latin and Asian text, Don't adjust space between Asian text and numbers

Deleted: <https://dst.gov.in/sites/default/files/Full%20Report%20%281%29.pdf>.

Formatted: Hyperlink, Font: +Body (Times New Roman), 11 pt,

Formatted: Font: +Body (Times New Roman), 11 pt,

Formatted: Indent: Left: 2.54 cm

538 **References**

539 Acreman, M. (2000). *Managed Flood Releases from Reservoirs: Issues and*
540 *Guidance.*
541 [https://sswm.info/sites/default/files/reference_attachments/ACREMAN%202000](https://sswm.info/sites/default/files/reference_attachments/ACREMAN%202000%20Managed%20Flood%20Releases%20from%20Reservoirs.pdf)
542 [%20Managed%20Flood%20Releases%20from%20Reservoirs.pdf](https://sswm.info/sites/default/files/reference_attachments/ACREMAN%202000%20Managed%20Flood%20Releases%20from%20Reservoirs.pdf)

Formatted: Font: 12 pt

543 [Agarwal, A., & Narain, S. \(1991\). *Floods, flood plains and environmental myths.*](#)

544 Ali, H., Modi, P., & Mishra, V. (2019). Increased flood risk in Indian sub-continent
545 under the warming climate. *Weather and Climate Extremes*, 25, 100212.
546 <https://doi.org/10.1016/J.WACE.2019.100212>

Formatted: Indent: Left: 2.54 cm

547 Allen, S. K., Linsbauer, A., Randhawa, S. S., Huggel, C., Rana, P., & Kumari, A.
548 (2016). Glacial lake outburst flood risk in Himachal Pradesh, India: an
549 integrative and anticipatory approach considering current and future threats.
550 *Natural Hazards*, 84(3), 1741–1763. <https://doi.org/10.1007/s11069-016-2511-x>

551 Apel, H., Aronica, G. T., Kreibich, H., & Thielen, A. H. (2009). Flood risk analyses -
552 How detailed do we need to be? *Natural Hazards*, 49(1), 79–98.
553 <https://doi.org/10.1007/S11069-008-9277-8/TABLES/5>

554 Bernhofen, M. V., Cooper, S., Trigg, M., Mdee, A., Carr, A., Bhave, A., Solano-
555 Correa, Y. T., Pencue-Fierro, E. L., Teferi, E., Haile, A. T., Yusop, Z., Alias, N.
556 E., Sa'adi, Z., Bin Ramzan, M. A., Dhanya, C. T., & Shukla, P. (2022). The
557 Role of Global Data Sets for Riverine Flood Risk Management at National
558 Scales. *Water Resources Research*, 58(4).
559 <https://doi.org/10.1029/2021wr031555>

560 Birkmann, J., & Welle, T. (2015). Assessing the risk of loss and damage: Exposure,
561 vulnerability and risk to climate-related hazards for different country
562 classifications. *International Journal of Global Warming*, 8(2), 191–212.
563 <https://doi.org/10.1504/IJGW.2015.071963>

566 Boulange, J., Hanasaki, N., Yamazaki, D., & Pokhrel, Y. (2021). Role of dams in
567 reducing global flood exposure under climate change. *Nature Communications*,
568 12(1). <https://doi.org/10.1038/s41467-020-20704-0>

569 [Brown, J. D., & Heuvelink, G. B. M. \(2005\). Assessing Uncertainty Propagation through](#)
570 [Physically Based Models of Soil Water Flow and Solute Transport. *Encyclopedia of*](#)
571 [Hydrological Sciences. <https://doi.org/10.1002/0470848944.HSA081>](#)

572 Chaudhari, S., & Pokhrel, Y. (2022). Alteration of River Flow and Flood Dynamics
573 by Existing and Planned Hydropower Dams in the Amazon River Basin. *Water*
574 *Resources Research*, 58(5). <https://doi.org/10.1029/2021WR030555>

575 [Cook, A., & Merwade, V. \(2009\). Effect of topographic data, geometric configuration and](#)
576 [modeling approach on flood inundation mapping. *Journal of Hydrology*, 377\(1–2\), 131–](#)
577 [142. <https://doi.org/10.1016/J.JHYDROL.2009.08.015>](#)

578 Dang, H., Pokhrel, Y., Shin, S., Stelly, J., Ahlquist, D., & Du Bui, D. (2022).
579 Hydrologic balance and inundation dynamics of Southeast Asia's largest inland
580 lake altered by hydropower dams in the Mekong River basin. *Science of The*
581 *Total Environment*, 831, 154833.
582 <https://doi.org/10.1016/J.SCITOTENV.2022.154833>

583 Dang, T. D., Chowdhury, A. K., & Galelli, S. (2019). On the representation of water
584 reservoir storage and operations in large-scale hydrological models:
585 implications on model parameterization and climate change impact assessments.
586 *Hydrology and Earth System Sciences Discussions*, 1–34.
587 <https://doi.org/10.5194/hess-2019-334>

588 de Moel, H., Jongman, B., Kreibich, H., Merz, B., Penning-Rowsell, E., & Ward, P.
589 J. (2015). Flood risk assessments at different spatial scales. *Mitigation and*
590 *Adaptation Strategies for Global Change*, 20(6), 865–890.
591 <https://doi.org/10.1007/s11027-015-9654-z>

592 [Dey, S., Saksena, S., Winter, D., Merwade, V., & McMillan, S. \(2022\). Incorporating Network](#)
593 [Scale River Bathymetry to Improve Characterization of Fluvial Processes in Flood](#)
594 [Modeling. *Water Resources Research*, 58\(11\), e2020WR029521.](#)
595 <https://doi.org/10.1029/2020WR029521>

596 Di Baldassarre, G., & Montanari, A. (2009). Uncertainty in river discharge
597 observations: A quantitative analysis. *Hydrology and Earth System Sciences*,
598 13(6), 913–921. <https://doi.org/10.5194/HESS-13-913-2009>

599 Dottori, F., Salamon, P., Bianchi, A., Alfieri, L., Hirpa, F. A., & Feyen, L. (2016).
600 Development and evaluation of a framework for global flood hazard mapping.
601 *Advances in Water Resources*, 94, 87–102.
602 <https://doi.org/10.1016/J.ADVWATRES.2016.05.002>

603 Eidsvig, U. M. K., Kristensen, K., & Vangelsten, B. V. (2017). Assessing the risk
604 posed by natural hazards to infrastructures. *Natural Hazards and Earth System*
605 *Sciences*, 17(3), 481–504. <https://doi.org/10.5194/nhess-17-481-2017>

Moved (insertion) [2]

Formatted: Indent: Left: 2.54 cm

Formatted: Indent: Left: 2.54 cm

Formatted: Indent: Left: 2.54 cm

606 [Fredrick, O. \(2017, May 19\). Excavators allege debris was used to bury storey in Chhatar](https://www.hindustantimes.com/lucknow/excavators-allege-debris-was-used-to-bury-storey-in-chhatar-manzil/story-mMm8Dwog3azR6SSEmpvjIO.html)
607 [Manzil. *Hindustan Times*. \[https://www.hindustantimes.com/lucknow/excavators-allege-\]\(https://www.hindustantimes.com/lucknow/excavators-allege-debris-was-used-to-bury-storey-in-chhatar-manzil/story-mMm8Dwog3azR6SSEmpvjIO.html\)](https://www.hindustantimes.com/lucknow/excavators-allege-debris-was-used-to-bury-storey-in-chhatar-manzil/story-mMm8Dwog3azR6SSEmpvjIO.html)
608 [debris-was-used-to-bury-storey-in-chhatar-manzil/story-](https://www.hindustantimes.com/lucknow/excavators-allege-debris-was-used-to-bury-storey-in-chhatar-manzil/story-mMm8Dwog3azR6SSEmpvjIO.html)
609 [mMm8Dwog3azR6SSEmpvjIO.html](https://www.hindustantimes.com/lucknow/excavators-allege-debris-was-used-to-bury-storey-in-chhatar-manzil/story-mMm8Dwog3azR6SSEmpvjIO.html)

610 Gaur, A., & Gaur, A. (2018). *Future Changes in Flood Hazards across Canada*
611 *under a Changing Climate*. <https://doi.org/10.3390/w10101441>

612 Ghosh, A., & Kar, S. K. (2018). Application of analytical hierarchy process (AHP)
613 for flood risk assessment: a case study in Malda district of West Bengal, India.
614 *Natural Hazards*, 94(1), 349–368. <https://doi.org/10.1007/s11069-018-3392-y>

615 Hanasaki, N., Kanae, S., Oki, T., Masuda, K., Motoya, K., Shirakawa, N., Shen, Y.,
616 & Tanaka, K. (2008). An integrated model for the assessment of global water
617 resources - Part 1: Model description and input meteorological forcing.
618 *Hydrology and Earth System Sciences*, 12(4), 1007–1025.
619 <https://doi.org/10.5194/HESS-12-1007-2008>

620 Hanasaki, N., Yoshikawa, S., Pokhrel, Y., & Kanae, S. (2018). A global hydrological
621 simulation to specify the sources of water used by humans. *Hydrology and*
622 *Earth System Sciences*, 22(1), 789–817. [https://doi.org/10.5194/hess-22-789-](https://doi.org/10.5194/hess-22-789-2018)
623 2018

624 [He, X., Bryant, B. P., Moran, T., Mach, K. J., Wei, Z., & Freyberg, D. L. \(2021\). Climate-](https://doi.org/10.1126/SCIADV.ABE6025/SUPPL_FILE/ABE6025_SM.PDF)
625 [informed hydrologic modeling and policy typology to guide managed aquifer recharge.](https://doi.org/10.1126/SCIADV.ABE6025/SUPPL_FILE/ABE6025_SM.PDF)
626 [Science Advances](https://doi.org/10.1126/SCIADV.ABE6025/SUPPL_FILE/ABE6025_SM.PDF), 7(17), 6025–6046.
627 https://doi.org/10.1126/SCIADV.ABE6025/SUPPL_FILE/ABE6025_SM.PDF

628 Hirabayashi, Y., Mahendran, R., Koirala, S., Konoshima, L., Yamazaki, D.,
629 Watanabe, S., Kim, H., & Kanae, S. (2013). Global flood risk under climate
630 change. *Nature Climate Change*, 3(9), 816–821.
631 <https://doi.org/10.1038/nclimate1911>

632 Hirabayashi, Y., Tanoue, M., Sasaki, O., Zhou, X., & Yamazaki, D. (2021). Global
633 exposure to flooding from the new CMIP6 climate model projections. *Scientific*
634 *Reports*, 0123456789, 1–7. <https://doi.org/10.1038/s41598-021-83279-w>

635 Hochrainer-Stigler, S., Schinko, T., Hof, A., & Ward, P. J. (2021). Adaptive risk
636 management strategies for governments under future climate and socioeconomic
637 change: An application to riverine flood risk at the global level. *Environmental*
638 *Science and Policy*, 125, 10–20. <https://doi.org/10.1016/j.envsci.2021.08.010>

639 Hooper, E., & Chapman, L. (2012). The impacts of climate change on national road
640 and rail networks. In *Transport and Sustainability* (Vol. 2, pp. 105–136).
641 Emerald Group Publishing Ltd. [https://doi.org/10.1108/S2044-](https://doi.org/10.1108/S2044-9941(2012)0000002008)
642 9941(2012)0000002008

643 Hu, P., Zhang, Q., Shi, P., Chen, B., & Fang, J. (2018). Flood-induced mortality
644 across the globe: Spatiotemporal pattern and influencing factors. *Science of The*
645 *Total Environment*, 643, 171–182.
646 <https://doi.org/10.1016/J.SCITOTENV.2018.06.197>

Formatted: Indent: Left: 2.54 cm

Formatted: Indent: Left: 2.54 cm

647 IPCC. (2014). *Climate Change 2014: Synthesis Report. Contribution of Working*
648 *Groups I, II, and III to the Fifth Assessment Report of the. Geneva, Switzerland:*
649 *Intergovernmental Panel on Climate Change.*

650 Jain, G., Singh, C., Coelho, K., & Malladi, T. (2017). *Long-term implications of*
651 *humanitarian responses The case of Chennai.*
652 <http://pubs.iied.org/10840IIEDwww.iied.org@iiedwww.facebook.com/theIIED>

653 Joint Research Centre (JRC), European Commission and Center for International
654 Earth Science Information Network (CIESIN), & Columbia University. (2021).
655 *Global Human Settlement Layer: Population and Built-Up Estimates, and*
656 *Degree of Urbanization Settlement Model Grid. Palisades, NY: NASA*
657 *Socioeconomic Data and Applications Center (SEDAC).*
658 <https://doi.org/10.7927/h4154f0w>

659 [Joshi, V. \(2014, September 14\). Have we learnt from past floods? Clearly not! Hindustan Times](https://www.pressreader.com/india/hindustan-times-lucknow/20140914/281646778342401)
660 [/Lucknow\). \[https://www.pressreader.com/india/hindustan-times-\]\(https://www.pressreader.com/india/hindustan-times-lucknow/20140914/281646778342401\)](https://www.pressreader.com/india/hindustan-times-lucknow/20140914/281646778342401)
661 [lucknow/20140914/281646778342401](https://www.pressreader.com/india/hindustan-times-lucknow/20140914/281646778342401)

662 Kalantari, Z., Briel, A., Lyon, S. W., Olofsson, B., & Folkesson, L. (2014). On the
663 utilization of hydrological modelling for road drainage design under climate and
664 land use change. *Science of the Total Environment*, 475, 97–103.
665 <https://doi.org/10.1016/J.SCITOTENV.2013.12.114>

666 Kimuli, J. B., Di, B., Zhang, R., Wu, S., Li, J., & Yin, W. (2021). A multisource trend
667 analysis of floods in Asia-Pacific 1990–2018: Implications for climate change in
668 sustainable development goals. In *International Journal of Disaster Risk*
669 *Reduction* (Vol. 59). Elsevier Ltd. <https://doi.org/10.1016/j.ijdr.2021.102237>

670 Koks, E. E., Rozenberg, J., Zorn, C., Tariverdi, M., Vousdoukas, M., Fraser, S. A.,
671 Hall, J. W., & Hallegatte, S. (2019). A global multi-hazard risk analysis of road
672 and railway infrastructure assets. *Nature Communications*, 10(1).
673 <https://doi.org/10.1038/s41467-019-10442-3>

674 Kushwaha, A. P., Tiwari, A. D., Dangar, S., Shah, H., Mahto, S. S., & Mishra, V.
675 (2021). Multimodel assessment of water budget in Indian sub-continental river
676 basins. *Journal of Hydrology*, 603, 126977.
677 <https://doi.org/10.1016/J.JHYDROL.2021.126977>

678 [Laiolo, P., Gabellani, S., Campo, L., Cenci, L., Silvestro, F., Delogu, F., Boni, G., Rudari, R.,](https://doi.org/10.1109/IGARSS.2015.7326015)
679 [Puca, S., & Pisani, A. R. \(2015\). Assimilation of remote sensing observations into a](https://doi.org/10.1109/IGARSS.2015.7326015)
680 [continuous distributed hydrological model: Impacts on the hydrologic cycle. *International*](https://doi.org/10.1109/IGARSS.2015.7326015)
681 [Geoscience and Remote Sensing Symposium \(IGARSS\), 2015-November, 1308–1311.](https://doi.org/10.1109/IGARSS.2015.7326015)
682 <https://doi.org/10.1109/IGARSS.2015.7326015>

683 Lehner, B., Liermann, C. R., Revenga, C., Vörösmarty, C., Fekete, B., Crouzet, P.,
684 Döll, P., Endejan, M., Frenken, K., Magome, J., Nilsson, C., Robertson, J. C.,
685 Rödel, R., Sindorf, N., & Wisser, D. (2011). High-resolution mapping of the
686 world's reservoirs and dams for sustainable river-flow management. In

Formatted: Font: Not Italic

Moved up [1]: K.

Deleted: Mintenbeck, A. Alegria, M. Craig, S. Langsdorf, S. Löschke, V. Möller, A. Okem,

Moved up [2]: B.

Deleted: IPCC. (2022). *Climate Change 2022: Impacts, Adaptation, and Vulnerability*. Contribution of Working Group II to the Sixth Assessment Report of the Intergovernmental Panel on Climate Change [H.-O. Pörtner, D.C. Roberts, M. Tignor, E.S. Poloczanska,

Deleted: Rama (eds.]). Cambridge University Press. Cambridge University Press, Cambridge, UK and New York, NY, USA, 3056 pp., doi:10.1017/9781009325844.¶

Formatted: Indent: Left: 2.54 cm

Formatted: Indent: Left: 2.54 cm

- 699 *Frontiers in Ecology and the Environment* (Vol. 9, Issue 9, pp. 494–502).
700 <https://doi.org/10.1890/100125>
- 701 Marchand, M., Dahm, R., Buurman, J., Sethurathinam, S., & Sprengers, C. (2022).
702 Flood protection by embankments in the Brahmani–Baitarani river basin, India:
703 a risk-based approach. *International Journal of Water Resources Development*,
704 38(2), 242–261. <https://doi.org/10.1080/07900627.2021.1899899>
- 705 Mateo, C. M., Hanasaki, N., Komori, D., & Tanaka, K. (2014). Assessing the impacts
706 of reservoir operation to floodplain inundation by combining hydrological,
707 reservoir management, and hydrodynamic models. *AGU Publications*, 7245–
708 7266. <https://doi.org/10.1002/2013WR014845>.Received
- 709 Mateo, C. M. R., Hanasaki, N., Komori, D., Yoshimura, K., Kiguchi, M.,
710 Champathong, A., Yamazaki, D., Sukhapunphan, T., & Oki, T. (2013). A
711 simulation study on modifying reservoir operation rules: Tradeoffs between
712 flood mitigation and water supply. *IAHS-AISH Proceedings and Reports*,
713 362(July), 33–40.
- 714 Mateo, C. M. R., Hanasaki, N., Komori, D., Yoshimura, K., Kiguchi, M.,
715 Champathong, A., Yamazaki, D., Sukhapunphan, T., & Oki, T. (2014). Flood
716 risk and climate change: global and regional perspectives. *Hydrological
717 Sciences Journal*, 59(1), 1–28. <https://doi.org/10.1080/02626667.2013.857411>
- 718 Mishra, D. K. (2015, March 10). 1948 Floods in Bihar-2 Inaugural flood after Independence –
719 Official Version of Floods and its Aftermath. *SANDRP*. [https://sandrp.in/2015/03/10/1948-
720 floods-in-bihar-2-inaugural-flood-after-independence-official-version-of-floods-and-its-
721 aftermath/](https://sandrp.in/2015/03/10/1948-floods-in-bihar-2-inaugural-flood-after-independence-official-version-of-floods-and-its-aftermath/)
- 722 [Mishra, V.](#), & Shah, H. L. (2018). Hydroclimatological Perspective of the Kerala
723 Flood of 2018. *Journal of the Geological Society of India*, 92(5), 645–650.
724 <https://doi.org/10.1007/s12594-018-1079-3>
- 725 Mishra, V., Tiwari, A. D., & Kumar, R. (2022). Warming climate and ENSO
726 variability enhance the risk of sequential extremes in India. *One Earth*, 5(11),
727 1250–1259. <https://doi.org/10.1016/J.ONEEAR.2022.10.013>
- 728 Mittal, N., Bhawe, A. G., Mishra, A., & Singh, R. (2016). Impact of human
729 intervention and climate change on natural flow regime. *Water Resources
730 Management*, 30(2), 685–699. <https://doi.org/10.1007/s11269-015-1185-6>
- 731 Mohanty, M. P., Mudgil, S., & Karmakar, S. (2020). Flood management in India: A
732 focussed review on the current status and future challenges. In *International
733 Journal of Disaster Risk Reduction* (Vol. 49). Elsevier Ltd.
734 <https://doi.org/10.1016/j.ijdr.2020.101660>
- 735 Mohapatra, P. K., & Singh, R. D. (2003). Flood management in India. *Natural
736 Hazards*, 28, 131–143. <https://doi.org/10.1177/0019556120120109>

Formatted: Indent: Left: 2.54 cm

- 737 Mukherjee, S., Aadhar, S., Stone, D., & Mishra, V. (2018). Increase in extreme
738 precipitation events under anthropogenic warming in India. *Weather and*
739 *Climate Extremes*, 20, 45–53. <https://doi.org/10.1016/J.WACE.2018.03.005>
- 740 Nanditha, J. S., Kushwaha, A. P., Singh, R., Malik, I., Solanki, H., Singh Chupal, D.,
741 Dangar, S., Shwarup Mahto, S., Mishra, V., Vegad, U., Chuphal, D. S., &
742 Mahto, S. S. (2022). The Pakistan flood of August 2022: causes and
743 implications. *Authorea Preprints*. <https://doi.org/10.1002/ESSOAR.10512560.1>
- 744 Nanditha, J. S., & Mishra, V. (2021). On the need of ensemble flood forecast in India.
745 *Water Security*, 12, 100086. <https://doi.org/10.1016/J.WASEC.2021.100086>
- 746 Nanditha, J. S., & Mishra, V. (2022). Multiday Precipitation Is a Prominent Driver of
747 Floods in Indian River Basins. *Water Resources Research*, 58(7),
748 e2022WR032723. <https://doi.org/10.1029/2022WR032723>
- 749 Nilsson, C., Catherine, *, Reidy, A., Dynesius, M., & Revenga, C. (2005).
750 Fragmentation and Flow Regulation of the World's Large River Systems. In
751 *SCIENCE* (Vol. 308). www.sciencemag.org
- 752 Padhra, A. (2022). Tourism in India and the Impact of Weather and Climate. In
753 *Indian Tourism* (pp. 187–197). Emerald Publishing Limited.
754 <https://doi.org/10.1108/978-1-80262-937-820221013>
- 755 Pai, D. S., Sridhar, L., Rajeevan, M., Sreejith, O. P., Satbhai, N. S., &
756 Mukhopadhyay, B. (2014). Development of a new high spatial resolution (0.25°
757 × 0.25°) long period (1901-2010) daily gridded rainfall data set over India and
758 its comparison with existing data sets over the region. *Mausam*, 65(1), 1–18.
- 759 Pathak, S., Liu, M., Jato-Espino, D., & Zevenbergen, C. (2020). Social, economic and
760 environmental assessment of urban sub-catchment flood risks using a multi-
761 criteria approach: A case study in Mumbai City, India. *Journal of Hydrology*,
762 591, 125216. <https://doi.org/10.1016/J.JHYDROL.2020.125216>
- 763 Peduzzi, P., Dao, H., Herold, C., & Mouton, F. (2009). Natural Hazards and Earth
764 System Sciences Assessing global exposure and vulnerability towards natural
765 hazards: the Disaster Risk Index. In *Hazards Earth Syst. Sci* (Vol. 9). [www.nat-](http://www.nat-hazards-earth-syst-sci.net/9/1149/2009/)
766 [hazards-earth-syst-sci.net/9/1149/2009/](http://www.nat-hazards-earth-syst-sci.net/9/1149/2009/)
- 767 Pekel, J. F., Cottam, A., Gorelick, N., & Belward, A. S. (2016). High-resolution
768 mapping of global surface water and its long-term changes. *Nature*, 540(7633),
769 418–422. <https://doi.org/10.1038/nature20584>
- 770 Pokhrel, Y., Shin, S., Lin, Z., Yamazaki, D., & Qi, J. (2018). Potential Disruption of
771 Flood Dynamics in the Lower Mekong River Basin Due to Upstream Flow
772 Regulation. *Scientific Reports*, 8(1). [https://doi.org/10.1038/s41598-018-35823-](https://doi.org/10.1038/s41598-018-35823-4)
773 [4](https://doi.org/10.1038/s41598-018-35823-4)
- 774 [Poulin, A., Brissette, F., Leconte, R., Arsenault, R., & Malo, J. S. \(2011\). Uncertainty of](#)
775 [hydrological modelling in climate change impact studies in a Canadian, snow-dominated](#)

776 [river basin. *Journal of Hydrology*, 409\(3–4\), 626–636.](#)
777 <https://doi.org/10.1016/J.JHYDROL.2011.08.057>

778 Rentschler, J., Salhab, M., & Jafino, B. A. (2022). Flood exposure and poverty in 188
779 countries. *Nature Communications*, 13(1). [https://doi.org/10.1038/s41467-022-](https://doi.org/10.1038/s41467-022-30727-4)
780 30727-4

781 Roxy, M. K., Ghosh, S., Pathak, A., Athulya, R., Mujumdar, M., Murtugudde, R.,
782 Terray, P., & Rajeevan, M. (2017). A threefold rise in widespread extreme rain
783 events over central India. *Nature Communications*, 8(1).
784 <https://doi.org/10.1038/s41467-017-00744-9>

785 Roy, B., Khan, M. S. M., Saiful Islam, A. K. M., Khan, M. J. U., & Mohammed, K.
786 (2021). Integrated flood risk assessment of the arial khan river under changing
787 climate using ipcc ar5 risk framework. *Journal of Water and Climate Change*,
788 12(7), 3421–3447. <https://doi.org/10.2166/wcc.2021.341>

789 Shah, H. L., & Mishra, V. (2016). Hydrologic Changes in Indian Subcontinental
790 River Basins (1901–2012). *Journal of Hydrometeorology*, 17(10), 2667–2687.
791 <https://doi.org/10.1175/JHM-D-15-0231.1>

792 Sheffield, J., Goteti, G., & Wood, E. F. (2006). *Development of a 50-Year High-*
793 *Resolution Global Dataset of Meteorological Forcings for Land Surface*
794 *Modeling*.

795 Singh, A., Mani, M., & Vishnoi, R. K. (2021). Tehri Dam—A Savior from Climate Change Led
796 Extreme Events. *INCOLD Journal (A Half Yearly Technical Journal of Indian Committee*
797 *on Large Dams)*, 10(2), 44–50.

798 [Singh, P., Sinha, V. S. P., Vijhani, A., & Pahuja, N. \(2018\). Vulnerability assessment](#)
799 [of urban road network from urban flood. *International Journal of Disaster Risk*](#)
800 [Reduction](#), 28, 237–250. <https://doi.org/10.1016/J.IJDRR.2018.03.017>

801 Smith, A., Bates, P. D., Wing, O., Sampson, C., Quinn, N., & Neal, J. (2019). New
802 estimates of flood exposure in developing countries using high-resolution
803 population data. *Nature Communications*, 10(1).
804 <https://doi.org/10.1038/s41467-019-09282-y>

805 Srivastava, A. K., Rajeevan, M., & Kshirsagar, S. R. (2009). Development of a high
806 resolution daily gridded temperature data set (1969 – 2005) for the Indian
807 region. *Atmospheric Science Letters*, 10(October), 249–254.
808 <https://doi.org/10.1002/asl>

809 Stephens, E. M., Bates, P. D., Freer, J. E., & Mason, D. C. (2012). The impact of
810 uncertainty in satellite data on the assessment of flood inundation models.
811 *Journal of Hydrology*, 414–415, 162–173.
812 <https://doi.org/10.1016/J.JHYDROL.2011.10.040>

813 Tanoue, M. (2020). *Future river-flood damage increases under aggressive*
814 *adaptations*. 1–12.

Formatted: Indent: Left: 2.54 cm

Formatted: Indent: Left: 2.54 cm

- 815 Teng, J., Jakeman, A. J., Vaze, J., Croke, B. F. W., Dutta, D., & Kim, S. (2017).
816 Flood inundation modelling: A review of methods, recent advances and
817 uncertainty analysis. *Environmental Modelling & Software*, *90*, 201–216.
818 <https://doi.org/10.1016/J.ENVSOFT.2017.01.006>
- 819 UNISDR. (2011). *Global Assessment Report on Disaster Risk Reduction 2011,*
820 *Revealing Risk, Redefining Development, United Nations International Strategy*
821 *for Disaster Reduction Secretariat, Geneva, 2011.*
822 https://www.undp.org/publications/2011-global-assessment-report-disaster-risk-reduction?utm_source=EN&utm_medium=GSR&utm_content=US_UNDP_PaidSearch_Brand_English&utm_campaign=CENTRAL&c_src=CENTRAL&c_src2=GSR&gclid=CjwKCAiAqaWdBhAvEiwAGAQlthTEIs1543d8ZuHyzCatyJutiZP2w2Wp41vZBSiouchJ7PvGpIcUBoCxOYQAvD_BwE
- 827 UNISDR. (2013). *Global Assessment Report on Disaster Risk Reduction 2013, From*
828 *Shared Risk to Shared Value: the Business Case for Disaster Risk Reduction,*
829 *United Nations International Strategy for Disaster Reduction Secretariat,*
830 *Geneva, 2013.* <https://www.undr.org/publication/global-assessment-report-disaster-risk-reduction-2013>
- 832 Varis, O., Taka, M., & Tortajada, C. (2022). Global human exposure to urban riverine
833 floods and storms. *River*. <https://doi.org/10.1002/rvr2.1>
- 834 Vu, D. T., Dang, T. D., Galelli, S., & Hossain, F. (2022). Satellite observations reveal
835 13 years of reservoir filling strategies, operating rules, and hydrological
836 alterations in the Upper Mekong River basin. *Hydrology and Earth System*
837 *Sciences*, *26*(9), 2345–2364. <https://doi.org/10.5194/hess-26-2345-2022>
- 838 Ward, P. J., Jongman, B., Weiland, F. S., Bouwman, A., Van Beek, R., Bierkens, M.
839 F. P., Ligtoet, W., & Winsemius, H. C. (2013). Assessing flood risk at the
840 global scale: Model setup, results, and sensitivity. *Environmental Research*
841 *Letters*, *8*(4). <https://doi.org/10.1088/1748-9326/8/4/044019>
- 842 Winsemius, H. C., Jongman, B., Veldkamp, T. I. E., Hallegatte, S., Bangalore, M., &
843 Ward, P. J. (2018). Disaster risk, climate change, and poverty: Assessing the
844 global exposure of poor people to floods and droughts. *Environment and*
845 *Development Economics*, *23*(3), 328–348.
846 <https://doi.org/10.1017/S1355770X17000444>
- 847 Winsemius, H. C., van Beek, L. P. H., Jongman, B., Ward, P. J., & Bouwman, A.
848 (2013). A framework for global river flood risk assessments. *Hydrology and*
849 *Earth System Sciences*, *17*(5), 1871–1892. <https://doi.org/10.5194/hess-17-1871-2013>
- 851 Yamazaki, D., De Almeida, G. A. M., & Bates, P. D. (2013). Improving
852 computational efficiency in global river models by implementing the local
853 inertial flow equation and a vector-based river network map. *Water Resources*
854 *Research*, *49*(11), 7221–7235. <https://doi.org/10.1002/wrcr.20552>

- 855 Yamazaki, D., Kanae, S., Kim, H., & Oki, T. (2011). *A physically based description*
856 *of floodplain inundation dynamics in a global river routing model.*
857 47(February), 1–21. <https://doi.org/10.1029/2010WR009726>
- 858 Yamazaki, D., Watanabe, S., & Hirabayashi, Y. (2018). Global Flood Risk Modeling
859 and Projections of Climate Change Impacts. *Global Flood Hazard: Applications*
860 *in Modeling, Mapping, and Forecasting*, 233, 185–203. [http://cmip-](http://cmip-pcmdi.llnl.gov/)
861 [pcmdi.llnl.gov/](http://cmip-pcmdi.llnl.gov/)
- 862 Yang, T., Sun, F., Gentine, P., Liu, W., Wang, H., Yin, J., Du, M., & Liu, C. (2019).
863 Evaluation and machine learning improvement of global hydrological model-
864 based flood simulations. *Environmental Research Letters*, 14(11).
865 <https://doi.org/10.1088/1748-9326/ab4d5e>
- 866 Zajac, Z., Revilla-Romero, B., Salamon, P., Burek, P., Hirpa, F., & Beck, H. (2017).
867 The impact of lake and reservoir parameterization on global streamflow
868 simulation. *Journal of Hydrology*, 548, 552–568.
869 <https://doi.org/10.1016/j.jhydrol.2017.03.022>
- 870 Zhao, F., Veldkamp, T. I. E., Frieler, K., Schewe, J., Ostberg, S., Willner, S.,
871 Schauburger, B., Gosling, S. N., Schmied, H. M., Portmann, F. T., Leng, G.,
872 Huang, M., Liu, X., Tang, Q., Hanasaki, N., Biemans, H., Gerten, D., Satoh, Y.,
873 Pokhrel, Y., ... Yamazaki, D. (2017). The critical role of the routing scheme in
874 simulating peak river discharge in global hydrological models. *Environmental*
875 *Research Letters*, 12(7). <https://doi.org/10.1088/1748-9326/aa7250>

876

Formatted: Left, None, Indent: Left: 1.69 cm, Hanging: 0.85 cm, Space Before: 0 pt, After: 10 pt, Line spacing: Multiple 1.15 li, Don't keep with next, Don't keep lines together, Don't hyphenate, Don't adjust space between Latin and Asian text, Don't adjust space between Asian text and numbers

Formatted: Font: +Body (Times New Roman), 11 pt, Not Bold,